

1 Riverine particulate C and N generated at the permafrost thaw front:
2 case study of western Siberian rivers across a 1700-km latitudinal transect

3
4 Ivan V. KRICKOV¹, Artem G. LIM¹, Rinat M. MANASYPOV^{1,2},
5 Sergey V. LOIKO¹, Liudmila S. SHIROKOVA^{2,3}, Sergey N. KIRPOTIN¹,
6 Jan KARLSSON⁴, Oleg S. POKROVSKY^{3*}

7
8 ¹ *BIO-GEO-CLIM Laboratory, Tomsk State University, Tomsk, Russia*

9 ² *N. Laverov Federal Center for Integrated Arctic Research, Russian Academy of Sciences,*
10 *Arkhangelsk, Russia*

11 ³ *Geosciences and Environment Toulouse, UMR 5563 CNRS, 14 Avenue Edouard Belin 31400*
12 *Toulouse, France*

13 ⁴ *Climate Impacts Research Centre, Department of Ecology and Environmental Science, Umeå*
14 *University, 901 87 Umeå, Sweden*

15
16 **Email: oleg.pokrovsky@get.omp.eu*

17 *Key words: nutrient, particulate, suspended, landscape, bog, lake, forest, thaw, Siberia*

18
19 Submitted to *Biogeosciences*, after revision, August 2018
20
21
22
23
24
25
26
27
28
29

30 **Abstract**

31 In contrast to numerous studies on the dynamics of dissolved ($< 0.45 \mu\text{m}$) elements in
32 permafrost-affected high latitude rivers, very little is known of the behavior of river suspended ($>$
33 $0.45 \mu\text{m}$) matter (RSM) in these regions. In order to test the effect of climate, permafrost and
34 physio-geographical landscape parameters (bogs, forest and lake coverage of the watershed) on
35 RSM and particulate C, N and P concentration in river water, we sampled 33 small and medium
36 size rivers (10 – 100,000 km^2 watershed) along a 1700 km N - S transect including both
37 permafrost-affected and permafrost-free zones of **the** Western Siberian Lowland (WSL). The
38 concentration of C and N in RSM decreased with the increase in river watershed size, illustrating
39 *i*) the importance of organic debris in small rivers which drain peatlands and *ii*) the role of mineral
40 matter from bank abrasion in larger rivers. The presence of lakes in the watershed increased C and
41 N but decreased P concentrations in **the** RSM. The C:N ratio in the RSM reflected the source
42 from deep rather than surface soil horizon, similar to that of other Arctic rivers. This suggests the
43 export of peat and mineral particles through suprapermafrost flow occurring at the base of the
44 active layer. There was a maximum of **both** particulate C and N concentration **and export fluxes**
45 at the beginning of permafrost appearance, **in the** sporadic and discontinuous zone (62-64°N). This
46 presumably reflected the organic matter mobilization from newly thawed organic horizons in soils
47 at the active latitudinal thawing front. The results suggest that a northward shift of permafrost
48 boundaries and an increase in active layer thickness may increase particulate C and N export by
49 WSL rivers to the Arctic Ocean by a factor of 2, while P export may remain unchanged. In
50 contrast, within a long-term climate warming scenario, the disappearance of permafrost in the
51 north, the drainage of lakes and transformation of bogs to forest may decrease C and N
52 concentration in RSM by 2 to 3 times.

53

54

1. Introduction

High-latitude rivers are most vulnerable to on-going climate change via altering their hydrological regime (Bring et al., 2016) and widespread permafrost thaw that stimulates nutrient release (Vonk et al., 2015). For carbon (C), the particulate fraction (POC) contributes substantially to the total organic C export from the continent to the ocean (Schlesinger and Melack, 1981; Lal, 2003; Ludwig and Probst, 1996; Galy et al., 2015; Li et al., 2017; Coppola et al., 2018); a two-fold increase of Arctic rivers POC fluxes by 2100 is predicted (Gordeev and Kravchishina, 2009). Although the reasons for strong variations of POC in freshwaters are not yet fully understood (Tiang et al., 2015; Lee et al., 2015; Yang et al., 2016), the temperature (Hilton, 2016) and runoff (Goni et al., 2015) combined with local storm events (Jeong et al., 2012; Wiegner et al., 2009) are widely recognized as the most important driving factors. This may be especially true for northern aquatic systems, being highly sensitive to flood events, due to shallow water paths and short transit time in watersheds.

Of special interest to POC of the Arctic rivers is that, if soil organic C escapes degradation during river transport and thus buried in marine sediments, it can contribute to a geological carbon dioxide sink (e.g., Hilton et al., 2015). Further, potentially increased transport of P and N may significantly change primary productivity in riverine ecosystems (Wrona et al. 2016; McClelland et al. 2007), thereby impeding rigorous predictions of climate change impact on Arctic terrestrial-aquatic ecosystems.

Despite significant efforts in characterizing the fluxes, chemistry, and origin of particulate organic matter (POM) in large Arctic Rivers (Lobbés et al., 2000; Dittmar and Kattner, 2003; Unger et al., 2005; Guo et al., 2004, Guo and Macdonald, 2006; Gladyshev et al., 2015; Emmerton et al., 2008; McClelland et al., 2016; Gareis and Lesack, 2017), these studies do not allow for assessment of mechanisms of POM generation in the watershed. In particular, the role of size of the river watershed and its landscape (physio-geographical) parameters is still poorly known.

80 Thus, although detailed studies of particulate nutrients in small Arctic rivers helped to constrain
81 seasonal features of export fluxes (Cai et al., 2008; Dornblaser and Striegl, 2007; Lamoureux and
82 Lafrenière, 2014; McClelland et al., 2014), the key environmental driving factors of particulate
83 nutrient concentration and stoichiometry in Arctic rivers—permafrost coverage and lakes and
84 forest proportion on the watershed—remain poorly resolved.

85 In this regard, large continental plains such as the western Siberia Lowland (WSL), which
86 contains sizeable reservoirs of frozen and thawed organic carbon, N, P and inorganic nutrients
87 (Sheng et al. 2004; Stepanova et al., 2015; Raudina et al., 2017), may be especially useful in
88 assessing environmental control on particulate nutrient transport to the Arctic Ocean. A vast
89 amount of frozen peat in this region can strongly affect the coastal Arctic system in the event of
90 permafrost thaw and enhanced RSM export from the watersheds. Due to the high homogeneity of
91 the WSL landscape, lithology, and topography, one can use the natural north-south gradient of the
92 permafrost zone distribution to assess the direct impact of permafrost conditions on river water
93 chemistry.

94 Detailed studies of the dissolved fraction of WSL river waters demonstrated several typical
95 features occurring over a sizeable gradient of climate and permafrost. In pioneering works of Frey
96 and co-workers it was shown that southern permafrost-free regions export 3 to 4 times greater
97 amounts of dissolved C, N and P (Frey and Smith, 2005; Frey et al., 2007a, b; Frey and
98 McClelland, 2009) and that wetlands exert a significant positive effect on carbon and nutrient
99 concentration in small rivers (Frey et al., 2007a; Frey and McClelland, 2009). Although the
100 majority of these features were confirmed by a more recent study of dissolved carbon and nutrients
101 in WSL rivers over main hydrological seasons (Pokrovsky et al., 2015 and Vorobyev et al., 2017,
102 respectively), an assessment of particulate load transport in WSL rivers has not yet been performed
103 and the mechanisms controlling particulate C, N and P mobilization from WSL soils to the Arctic
104 Ocean remain unknown.

105 To improve current understanding of magnitude and seasonality of riverine particulate
106 nutrient export, we quantified concentrations of C and macro- (N, P) nutrients across a vast
107 latitudinal gradient (1700 km) with special emphasis **on the** permafrost-bearing zone during three
108 main hydrological regimes: 1) the peak of spring flood (early June 2016), 2) the summer base flow
109 (August 2016), and 3) the autumn high flow before the ice (October 2016). We aimed at
110 **characterizing** the effect of latitude, permafrost coverage and fundamental landscape features
111 (proportion of bogs, lakes and forest in the watershed) as well as the size of the river itself on
112 particulate C, N and P concentration and the relative fraction of particulate versus total (particulate
113 + dissolved) nutrient transport. We further used acquired knowledge to infer the basic mechanisms
114 of particulate nutrient mobilization from soils to rivers and applied these mechanisms **to predict**
115 **change in** particulate nutrient concentration under climate warming, landscape evolution and
116 progressive permafrost thaw in the largest frozen peatland province in the world.

117

118 **2. Study Site and Methods**

119 The rivers were sampled in the Western Siberia Lowland (WSL), a huge (> 2 million km²),
120 peatland and forest zone situated in the taiga forest, forest-tundra and tundra zone. The position
121 of biomes follows the decrease of mean annual air temperature (MAAT) from -0.5°C in the south
122 to -9.5°C in the north. The permafrost distribution also follows the latitudinal gradient of MAAT
123 and changes from absent, isolated and sporadic in the south to discontinuous and continuous in
124 the north. Further details of WSL physio-geographical settings, peat and lithological description
125 of the territory are provided elsewhere (Kremenetski et al., 2003; Stepanova et al., 2015;
126 Pokrovsky et al., 2015; Raudina et al., 2017). For each biome (taiga, forest-tundra and tundra)
127 several rivers with different watershed sizes were chosen and **the** sampling **campaign** was
128 performed along a latitudinal transect following previous strategies for **WSL river dissolved load**
129 (Pokrovsky et al., 2015, 2016; Vorobyev et al., 2017).

130 Altogether, we sampled 33 rivers that belong to watersheds of Ob, Pur and Taz including
131 these large rivers as well (**Fig. 1**). The landscape parameters of sampled catchments were
132 determined by digitizing available soil, vegetation, lithological and geocryological maps (**Table**
133 **S1** and Vorobyev et al., 2017). There was no covariation between river size and other landscape
134 parameters including permafrost coverage. Sampling was performed during three main
135 hydrological seasons: 1) spring flood (17 May – 15 June 2016), 2) summer baseflow (1 – 29
136 August 2016), and 3) autumn baseflow before ice (24 September – 13 October 2016). Note that
137 the most interesting period—in terms of soil connection to the rivers—occurred in late autumn
138 when the active layer depth was at its maximum. This period has not been covered in previous
139 studies of dissolved WSL river load. The reason of sampling both summer and autumn period is
140 to test the role of connectivity between soil fluids and the rivers. In fact, the main factor controlling
141 elemental behavior during accelerating permafrost thaw and release of dissolved and particulate
142 C and nutrients to surrounding aquatic landscapes is the connectivity between soils and rivers or
143 lakes, which occurs via water and solute transport along the permafrost table (“supra-permafrost
144 flow”). The supra-permafrost (shallow subsurface) water occurs in the active layer, typically at
145 the border between the thawed and frozen part of the soil profile (Woo, 2012). In the frozen
146 peatbogs of WSL, the active (unfrozen) layer thickens (ALT) is maximal at the end of unfrozen
147 season, which is typically end of September - beginning of October (Raudina et al., 2018).

148 The sampling strategy consisted of moving from south to north in spring and autumn over
149 a 2-3 week period, following the natural change of seasons. This allowed us to sample all rivers
150 of the transect at approximately the same time after ice off and before ice on. The year 2016 was
151 normal for western Siberia in terms of spring, summer and autumn precipitation but the
152 temperature was 4 and 2.7 °C higher than normal spring and summer, respectively, and not
153 different from the average T in autumn (Rosgidromet, 2017). For assessing inter-annual variations
154 in RSM concentrations, we analyzed the RSM samples collected in WSL rivers across the same

155 transect during a previous campaign in the spring of 2014 and 2015 and the summer and autumn
156 of 2014 and 2015.

157 Large water samples were collected from the middle of the river at 0.5 m depth in pre-
158 cleaned polypropylene jars (30 to 50 L) and were allowed to decantate over 2-3 days. The water
159 of the bottom layer of the barrels (approx. 30% of the initial volume) was centrifuged on-site for
160 20 min at 3500 rpm using 50-mL Nalgene tubes; sediment was frozen at -18°C and freeze-dried
161 later in the laboratory. In addition to decantation and centrifugation, RSM was collected via direct
162 filtration of large volumes (20 to 30 L) of river water with an Inox (AISI 304) Teflon® PTFE-
163 coated filtration unit (Fisher Bioblock) equipped with 142 mm acetate cellulose Sartorius
164 membranes (0.45 µm) and operated at 5-7 bars. An average flow rate of 1-2 L h⁻¹ was created by
165 a peristaltic pump (MasterFlex B/T) with Teflon tubing. For determination of total concentration
166 of suspended material, smaller volumes of freshly collected river water (1-2 L) were filtered on-
167 site (at the river bank or in the boat) with pre-weighted acetate cellulose filters (47 mm, 0.45 µm)
168 and Nalgene 250-mL polystyrene filtration units using a Mityvac® manual vacuum pump.

169 There was reasonably good agreement, typically within 10%, between the concentration
170 of RSM collected in large barrels via decantation followed by centrifugation, a direct high-
171 pressure filtration using 142-mm membranes and vacuum filtration using Nalgene 250-mL unit.
172 The agreement was better than ±10% for large rivers in summer and autumn when the mineral
173 component dominated the RSM. The difference between two methods was between 10 and 20%
174 for small organic-rich rivers containing peat and plant debris especially in spring.

175 The C and N concentration in RSM collected from large-volume separation procedure was
176 measured using catalytic combustion with Cu-O at 900°C with an uncertainty of ≤ 0.5% using
177 Thermo Flash 2000 CN Analyzer at Tomsk University. The samples were analyzed before and
178 after 1:1 HCl treatment to distinguish between total and inorganic C; however the ratio of C_{organic}
179 : C_{carbonate} in RSM was always above 20 and the contribution of carbonate C to total C in the RSM

180 was equal in average $0.3 \pm 0.3\%$ (2 s.d., $n = 30$). In addition to RSM, we compared total and HCl-
181 treated C analysis in peat soil column (organic part and 3 separate mineral horizons) sampled from
182 the middle part of river transect. The $C_{\text{carbonate}}$ share was below 2 % of total C content for both the
183 mineral and organic part of soil columns. The analyses we performed could not distinguish mineral
184 N linked to clays (NH_4^+ cation) and organic N in the RSM. For P, the RSM samples were subjected
185 to full acid leaching in a clean room following ICP-MS (Agilent 7500 ce) analyses using methods
186 for C_{org} -rich natural samples described by Stepanova et al. (2015). Water samples for DOC and
187 total dissolved phosphorus (P_{tot}) were filtered on-site through $0.45 \mu\text{m}$ acetate cellulose filters
188 (Millipore, Sartorius) and analyzed following methods previously described by Pokrovsky et al.
189 (2015, 2016).

190 A regression analysis was used to quantify the relationship between C, N and P
191 concentration in RSM and the % of permafrost, wetlands, lake and forest coverage of the
192 watershed as well as the surface area of the watershed ($S_{\text{watershed}}$). In order to assess a general
193 impact of the permafrost on RSM nutrient concentration we separated all sampled rivers into five
194 categories according to the permafrost distribution on their watersheds: 1) permafrost-free (south
195 of 61°N), 2) isolated (61 to 63.5°N); 3) sporadic (63.5 to 65°N); 4) discontinuous (65 to 66°N),
196 and 5) continuous permafrost zones (north of 66°N). The non-parametric statistics were used
197 because, based on Shapiro-Wilk test of the normality of variables, the data on C, N, P
198 concentration in RSM and the % of element in suspended form were not normally distributed. For
199 these reasons, we used the median, 1st and 3rd quartiles to trace dependence of nutrient
200 concentration to the type of permafrost distribution. The differences in suspended C, N and P
201 concentration between different seasons and between each two adjacent permafrost zones were
202 tested using a Mann-Whitney U test for a paired data set with significance level at 0.05. For
203 unpaired data, a non-parametric H-criterion Kruskal-Wallis test was performed for all watershed
204 sizes and all permafrost zones.

205 3. Results

206 3.1. C, N and P concentrations in RSM and their link to seasons and watershed size

207 Mean bulk RSM concentration in the WSL river waters did not depend on the **season of**
208 **open-water period of the year** and was equal to 7.1 ± 3.9 , 8.1 ± 4.1 , and 7.0 ± 3.7 mg/L in spring,
209 summer and autumn, respectively (**Table 1**). The RSM concentrations weakly depended on the
210 size of the watersheds ($S_{\text{watershed}}$) with a negative relationship in autumn ($R^2 = 0.33$, $p < 0.05$, Fig.
211 **S1 A**). Further, the RSM concentration increased with permafrost coverage and latitude ($R^2 = 0.56$
212 and 0.41), although this was visible only in autumn (**Fig. S1 B, C, Table S2**). The sporadic
213 permafrost zone exhibited the highest RSM concentration in summer (**Fig. S1 D**). Finally, there
214 was no correlation ($p > 0.05$) between lake, bog or forest coverage and the RSM concentration
215 ($R^2 < 0.2$, see also **Table S2**). For RSM concentration, statistically significant difference between
216 different permafrost zones, notably between permafrost-free and permafrost-bearing regions, were
217 evidenced in summer and autumn using Kruskal-Wallis and Mann-Whitney tests (**Table S3**).

218 The concentrations of C, N and P in WSL rivers averaged over 3 seasons were equal to
219 $15.3\pm 9.7\%$, $1.2\pm 0.9\%$, and $0.49\pm 0.42\%$ in mass of RSM (1.05 ± 0.805 , 0.083 ± 0.066 , and
220 0.035 ± 0.036 mg L⁻¹ in the riverwater). The watershed size sizably affected the C concentration:
221 there was a power-law decrease of C with the size of watershed ($R^2 = 0.28$, 0.47, and 0.25 in
222 spring, summer and autumn, respectively **Fig. 2A**) but there was no relationship with the N and P
223 concentrations in RSM ($R^2 < 0.2$, **Fig. 2 B, C**). Generally, a 2 to 3-fold **decrease** in C_{org} , from ca.
224 20-30% in rivers with $S_{\text{watershed}} < 100$ km² to $C_{\text{org}} = 5-10\%$ in rivers with $S_{\text{watershed}} > 10,000$ km²
225 was observed. The C:N ratio of RSM was independent on the watershed size in spring but
226 decreased 2-3 times with $S_{\text{watershed}}$ increase ($R^2 = 0.4$) in summer and autumn (**Fig. 2D**).

227 The inter-annual variations of suspended nutrient concentration in WSL rivers were of
228 secondary order importance when compared to season and watershed size control. We did not find
229 any inter-annual differences (at $p < 0.05$) in RSM concentration and P concentration in RSM

230 collected in June and August in 2014, 2015, and 2016 for the same 8 rivers (Agan, Trom'egan,
231 Pyakopur, Aivasedapur, Purpe, Yamsovery, Pur and Taz, **Table S1**)

232

233 *3.2. Role of permafrost distribution and landscape parameters for C, N, and P* 234 *concentration and fraction of particulate nutrients*

235 There was a local maximum of C and N concentration in isolated and sporadic permafrost
236 zone (**Fig. 3 A, B, D, E**), which was not seen for P (**Fig. 4 C, F**). Overall, the differences in C and
237 N concentrations in RSM among different permafrost zones were significant as verified by the
238 non-parametric Kruskal-Wallis H-test ($0.005 < p < 0.05$), while the difference in P concentration
239 between permafrost zones was not significant ($p > 0.05$, see **Table S3 C, D**). Specifically, the C
240 demonstrated a maximum concentration (significant at $p < 0.02$ during all three seasons) at 62-
241 64°N (**Fig. S2 A**). The latitude generally did not impact N and P concentration in RSM (**Fig. S2**
242 **B, C**). **Significant** differences between adjacent permafrost zones were evidenced by C and N in
243 summer and autumn (**Table S3 D**).

244 The landscape parameters **of** the watershed (bogs, lakes and forest coverage) sizably
245 affected ($p < 0.05$) suspended C and N. Bogs and lakes **in** the watershed increased the
246 concentration of C and N in RSM whereas forest generally decreased C in RSM (**Fig. 4 A-B-C**
247 **for C, and Fig. S3 A-B-C for N**). This increase in C and N % with bogs and lakes coverage and
248 a decrease with forest presence was mostly visible in summer and autumn. The increase in lake
249 coverage of the watershed led to a decrease in P concentration in RSM in summer and autumn (R^2
250 = 0.31 and 0.22, respectively, **Fig. S3 D-E-F**) that was especially visible in autumn in the
251 permafrost-free zone ($R = -0.88$, **Table S2**). During this period, the P concentration in RSM
252 positively correlated with the presence of forest in the permafrost zone ($R = 0.60$, **Table S2**).

253 The Mann Whitney U-test for the impact of watershed parameters demonstrated significant
254 differences in C and N concentration (all seasons) and P concentration (summer baseflow)

255 between watersheds having < 10% and > 10% lake coverage, **Table S3-E**. The differences were
256 also observed among watershed with < 50% and > 50% of bogs for C (all seasons) and N (summer
257 and autumn), **Table S3-F**. Finally, the forest coverage (< 30% and > 30%) exhibited significant
258 effect on C and N (all seasons) and P (autumn baseflow), **Table S3-G**.

259 The share of particulate carbon versus total (dissolved + particulate C) did not demonstrate
260 any significant dependence on $S_{\text{watershed}}$, bogs, forest and permafrost proportions on the watershed
261 ($R^2 < 0.3$, not shown). However, there was a localized maximum of particulate carbon fraction
262 around 64°N within the isolated to sporadic permafrost zone (**Fig. 5 A and C**). The presence of
263 lakes sizably increased the particulate over total transport of C in rivers ($R^2 = 0.52$ and 0.32 in
264 spring and summer, respectively, **Fig. 5 B**). The share of particulate phosphorus versus total
265 ranged from 10 to 90%. It did not demonstrate any link to size of river watershed, % of forest and
266 bogs, and type of permafrost distribution (not shown).

267

268 *3.3.C, N, P and RSM export fluxes by WSL rivers*

269 Based on available hydrological data, we calculated open water-period fluxes of C, N and
270 P in WSL rivers. This analysis takes into account the spatial and temporal variability of river
271 discharge, performed using hydrological approaches elaborated for the dissolved (< 0.45 μm)
272 fraction of the river water (Pokrovsky et al., 2015, 2016). The seasonal fluxes of C, N, P and RSM
273 export by WSL rivers were calculated separately for spring (May and June), summer (July, August
274 and September) and autumn period (September-October) for each 2° - wide latitudinal belt of the
275 full WSL territory, following the approach developed for dissolved C and major and trace
276 elements in the river water (**Fig. S4**). These 3 seasons of open-water period represent by far the
277 largest contribution to overall annual element and RSM yield, following the results for other Arctic
278 rivers (McClelland et al., 2016). Thus, 6 ice-covered months (November to April) represent only
279 12% of annual POC export flux by the Ob River. Based on results of 3 main seasons, an open-

280 water period export fluxes of C, N, P and RSM were calculated (**Fig. 6**). There is a clear maximum
281 of C and N export fluxes at the beginning of permafrost appearance, in isolated to sporadic
282 permafrost zone. The obtained particulate C and N yields are comparable with other Siberian
283 rivers. For two largest WSL rivers, Pur and Taz, we found May to October export fluxes of 69 and
284 80 kg C km² y⁻¹ which is lower than the annual POC yield of the Ob River (191 kg C km⁻² y⁻¹) but
285 similar to that of the Yenisey River (103 kg C km⁻² y⁻¹), McClelland et al. (2016).

286

287 4. Discussion

288 4.1. Concentrations of C, N and P in the RSM and impact of the watershed size

289 The RSM values in WSL rivers (2 to 18 mg/L) are similar to other boreal rivers of low
290 runoff which drain peatlands such as Severnaya Dvina (2.3 to 16 mg/L; Pokrovsky et al., 2010)
291 but lower than the Ob River itself (around 30 mg/L; Gebhardt et al., 2004) and other big rivers of
292 the Kara Sea basin (average 22 mg/L; Gordeev et al., 1996). The POC values of the WSL rivers
293 (0.5 to 3.0 mg/L POC) are consistent with recent data on WSL river transects sampled in 2015
294 (Vorobyev et al., 2017) and are in agreement with those of the Ob-Taz River confluence measured
295 in June (1.3 mg/L; Gebhardt et al., 2004), the Ob River at Salekhard in May through October (0.8
296 to 2.4 mg POC/L; Le Fouest et al., 2013), the low reaches of the Ob River (1.2 to 2.4 mg POC/L;
297 McClelland et al., 2016), the mean multi-annual values of POC in subarctic rivers of Northern
298 Eurasia draining peatlands (3.2, 0.3, 0.9 mg POC/L for S. Dvina, Pechora and Ob as compiled in
299 Gordeev et al., 1996) and the Lena River basin (0.5 mg/L; Kutscher et al., 2015).

300 However, the C_{org} concentrations in RSM of WSL rivers (5 to 40%), notably in small and
301 medium size (< 10,000-100,000 km²) ones, are an order of magnitude higher than those in other
302 world rivers which drain mineral substrates (typically 1% C_{org} in RSM; Meybeck, 1993) and
303 significantly higher than the values of the Siberian rivers (2.3, 3.6, 5.8, 3.0% for Ob, Yenisey,
304 Lena and Kolyma, respectively; Gordeev and Kravchishina, 2009). For example, typical
305 concentration of C_{org} in RSM of large (S_{watershed} > 100,000 km²) Central Siberian rivers that drain

306 larch forest is only 0.4 to 0.5 % (Pokrovsky et al., 2005). The C_{org} concentration in the RSM of
307 Severnaya Dvina River (which has sizeable proportion of bogs and lakes within its watershed
308 compared to WSL rivers) is $2.7 \pm 0.7\%$ in May and $4.8 \pm 1.1\%$ in August (Savenko et al., 2004). The
309 N_{org} content in RSM ranges from 0.3 to 1.8 % (0.05 to 0.2 mg particulate N_{tot}/L) which is much
310 higher than that in sedimentary rocks (0.05 to 0.06 %; Houlton et al., 2018) but is comparable with
311 the value reported for the freshwater part of Ob river estuary (0.16 mg N/L; Gebhardt et al., 2004),
312 the Ob River at Salekhard in May to October (0.1 to 0.3 mg PON/L; Le Fouest et al., 2013), the
313 Yukon River (0.14 ± 0.09 mg particulate N/L; Guo and MacDonald, 2006), and small rivers of the
314 North slope of Alaska (0.05 to 0.6 mg PON/L; McClelland et al., 2014).

315 High concentrations of C (and N) in the RSM of WSL rivers may stem from the organic
316 nature of soils that prevail on river watersheds. The Histosols, one of the dominant soil groups of
317 WSL, are capable of providing a sizeable amount of organic particles given the higher
318 susceptibility of peat to physical disintegration compared to mineral soils. The enrichment of the
319 river water in C-rich particles may occur at both the river bank (especially in small rivers flowing
320 through the wetlands) and within the extensive floodplains via remobilization of organic-rich
321 sediments during high flow periods.

322 The concentration of C and N in RSM decreased with increase in $S_{watershed}$, thereby
323 illustrating the importance of organic particles in small rivers draining peatlands and the role of
324 mineral matter from bank abrasion in larger rivers. The impact of watershed size is more
325 significant for C than for N. Presumably this is because N is more affected by autochthonous
326 processes and that particulate N may partly be generated from phytoplankton and macrophytes in
327 the river. Small rivers ($S_{watershed} < 100-1000$ km²) exhibited the largest scatter in particulate C, N
328 (and P) concentrations. This is probably due to multiple sources of POM and the very short transit
329 time in the watershed that results in fast responses of river particulate load to minor variations in
330 surface hydrology including high sensitivity to local storm events.

331 The decrease of C:N in the RSM from small to large rivers likely reflected a shift in main
332 origin of suspended matter, from peat in small rivers to more lithogenic (deep soil) in large rivers.
333 This was mostly visible in summer and autumn; in spring the rivers exhibited a very homogeneous
334 C:N signature which may be linked to a dominant source of RSM from bank abrasion and sediment
335 transport as well as deposition within the riparian zone. In fact, the flood plain of the Ob river and
336 other rivers of the WSL extend more than 10 times the width of the main channel (Vorobyev et
337 al., 2015). Note that the C:N ratio in large rivers (>100,000 km²) approaches that of average
338 sedimentary rocks (8.1; Houlton et al., 2018). In this regard, highly homogeneous C:N ratios in
339 particulate load of Arctic rivers (7 to 18 for Mackenzie, Yukon, Kolyma, Lena, Yenisey and Ob
340 regardless of season; McClelland et al., 2016) are interpreted as the mixture of deep soil sources
341 where C:N < 10 (Schädel et al., 2014) and upper organic-rich horizons of soils with elevated C:N
342 (Gentsch et al., 2015). The Ob River demonstrates the youngest POC of all Arctic Rivers (-203
343 to -220 ‰ $\Delta^{14}\text{C}$; McClelland et al., 2016) which certainly indicates a relatively fresh (ca. 1,000-
344 2,000 years old) origin of particulate carbon that is presumably from intermediate peat horizons.

345 We believe that variations in C:N in RSM reflect different sources of organic material
346 feeding the river depending on seasons and latitudes. A compilation of C:N ratios in peat and
347 mineral horizons as well as in thermokarst lake sediments for four main sites of latitudinal transect
348 considered in this study is given in Fig. S5 of Supplement. The range of C:N values in RSM
349 rivers (10 to 20) is closer to that in sediments of thermokarst lakes (20 to 30). Note that the
350 resuspension of sediments may be an important source of water column POC (Yang et al., 2016).
351 The minerotrophic bogs, which are mostly linked to rivers via hydrological networks, have a C:N
352 ratio in upper peat horizons ranging from 24 to 28. In mineral soils of the region, the C:N range is
353 between 10 and 15 regardless of latitude, from the tundra situated Taz River riparian zone to the
354 taiga situated middle channel of the Ob River. For upper organic horizons the C:N is always higher
355 than the bottom mineral horizons. The old alluvial deposits of the Pyakopur River (discontinuous

356 permafrost zone) had only 0.2% of POC with C:N equal to 6. Overall, there is an enrichment in N
357 relative to C in the course of water transport of organic and organo-mineral solid particles from
358 soils and riparian deposits to the river water.

359

360

361 *4.2. A maximum of C and N in the isolated/sporadic permafrost zone and the impact of* 362 *river watershed characteristics*

363 Complementary to previous results on dissolved (< 0.45 µm) C and N concentrations in WSL
364 rivers acquired by Frey et al. (2007a) and Vorobyev et al. (2017) that demonstrated weak or no impact
365 of permafrost on DOC and DON, the particulate C and N were affected by the presence of permafrost
366 in summer and autumn but not affected by its presence in spring. Moreover, during freshet the
367 permafrost distribution did not influence the bulk RSM concentration in WSL rivers. This strongly
368 implies that the delivery of RSM in rivers, and its chemical composition, are tightly linked to the
369 thickness of the active layer and limited by transport of soil particles over the suprapermafrost flow
370 to the river channel. This thickness is highest in September at the end of the active season. In
371 agreement with this, the C and N demonstrated a maximum concentration and export fluxes at 62-
372 64°N, in the sporadic to isolated permafrost zone and was most visible during summer and autumn
373 (Fig. 3 A, B and 6 A, B). This latitudinal belt can be considered as a large-scale thawing front for
374 the frozen peat which corresponds to the southern boundary of permafrost persistence. It is
375 important to note that that WSL rivers exhibit maximum CO₂ emission fluxes at the sporadic to
376 isolated permafrost belt (Serikova et al., 2018), which could be linked to strong processing of POC
377 and PON in the water column of WSL rivers. Interestingly, that rate of POC biodegradation,
378 leading to potential CO₂ emissions, sizably exceeds that of DOC in boreal humic waters
379 (Attermeyer et al., 2018). Furthermore, a maximum percentage of particulate C over total C
380 (suspended + dissolved) was also in the isolated and sporadic permafrost zones in spring; this

381 maximum shifted to the sporadic permafrost zone in summer and moved northward to the
382 discontinuous permafrost zone in autumn (**Fig. 5 C**). We believe that this corresponds to a
383 progressive increase in the thickness of the active layer which controls the degree of peat and
384 mineral particles leaching from the soil profile to the river. The thickness of this layer increases
385 from spring to autumn and more importantly it moves northward during this period (Trofimova
386 and Balybina, 2014). Enhanced mobilization of nutrients at the “hot spot” of permafrost thaw in
387 frozen peat landscapes was recently demonstrated on a local scale in western Siberia (Loiko et al.,
388 2017).

389 The impact of watershed characteristics on particulate C and N was clearly pronounced
390 with increased C and N concentration in RSM where there were increased bog and lake
391 proportions and decreased C and N concentration where there was increasing forest coverage. The
392 stronger impact of lakes compared to bogs on C concentration in RSM suggests that the generation
393 of C-rich particles occurs more efficiently in large water bodies than in stagnant shallow water
394 bodies. Several mechanisms are likely to operate in this regard. First, photodegradation of DOM
395 in large and shallow lakes of WSL is expected to be quite strong similar to shallow Canadian thaw
396 ponds (Laurion and Mladenov, 2013). Additionally, given the very short transit time of water from
397 the surrounding peat to the lakes via suprapermfrost flow (Ala-aho et al., 2018a, b; Raudina et
398 al., 2018), the allochthonous chromophoric DOM-rich material that arrives to the lakes is
399 subjected to fast degradation and coagulation such as that shown in Scandinavian lakes
400 (Kortelainen et al., 2006b; von Wachenfeldt and Tranvik, 2008). Second, the peat abrasion at the
401 border of the thermokarst lakes and thaw ponds, which are highly abundant in the territory
402 (Polishchuk et al., 2017, 2018), occurs due to wave erosion and thermo-abrasion (Shirokova et al.,
403 2013; Manasypov et al., 2015). Physical disintegration of peat at the lake coast likely generates a
404 large amount of suspended organic-rich material that can be exported to hydrological networks
405 during, for example, lake drainage or through already existing connecting channels (Kirpotin et

406 al., 2008, 2011). Note that the maximal lake coverage of the WSL territory is in the 63°N to 64°N
407 latitudinal belt (Polishchuk et al., 2017) where maximum C and N concentration and RSM export
408 fluxes also occur. Because the majority of thermokarst lakes are isolated water bodies without
409 inlet and outlet, this connectivity is achieved via water movement along the permafrost table in
410 the thawed active layer (Raudina et al., 2018) in the form of so-called suprapermafrost flow
411 between peat bogs, lakes, and rivers.

412 Finally, for particulate P, neither its concentration nor the particulate fraction were affected
413 by permafrost distribution, probably due to the various processes of biological uptake and mineral
414 precipitation controlling P removal both in soil profile and in the river water. For example, lakes
415 and bogs retained particulate P, similar to that of dissolved P, which is in agreement with global
416 assessments (Bouwman et al., 2013), P behavior in European northern wetlands and lakes (Lidman
417 et al., 2014), and recent results on dissolved P in the WSL rivers (Vorobyev et al., 2017).

418

419 *4.3. Mechanisms of RSM generation and prospective for climate warming in western Siberia*

420 A framework of particulate C, N and P generation in WSL rivers across the permafrost
421 gradient is shown in **Fig. 7**. We suggest that the concentration **and export fluxes** of suspended
422 particles depends on both the supply and losses in the catchments. The sources of suspended
423 particles in WSL rivers include: (i) vegetation litter which is washed by surficial flow to the river,
424 especially in spring; (ii) surface (peat) soil horizons, which are also most active in spring,
425 especially in the north; (iii) deep peat and mineral horizons which provide the particles via bank
426 abrasion in spring and via suprapermafrost flow in summer and autumn, (iv) lake **and pond**
427 sediments formed either by flocculation of DOM via photo- and bio-degradation processes or via
428 lake coastal abrasion due to wave erosion, and finally, (v) autochthonous organic debris of
429 macrophytes, periphyton and phytoplankton, whose contribution is maximal in summer and
430 autumn. A non-steady-state physical erosion of peat soils in WSL provides maximum particulate

431 nutrients within the most fragile zone of actively thawing permafrost between 62 and 64°N of the
432 sporadic to isolated permafrost zone. The maximal thickness of the active layer progressively
433 moves north during the active season thereby leading to maximal export of particulate C, N, and
434 P at the thawing front. However, we also suggest that part of the differences in mobilized
435 particulates is masked by retention in recipient waters. The transit time of water and particles in the
436 southern WSL rivers is much longer than that in northern rivers (Ala-aho et al., 2018a, b) hence the
437 biological uptake mechanisms together with physio-chemical processes such as photo-degradation
438 of POC (Mayer et al., 2006; Riggsbee et al., 2008) or cryocoagulation (Pokrovsky et al., 2018) have
439 sufficient time to act on suspended matter of soil and shallow subsurface waters and to remove the
440 nutrients from the river water as well. In rivers of the continuous permafrost zone, a relatively small
441 stock of nutrient-rich particles within the soil profile and on soil surface (as plant litter) is largely
442 compensated for by a more rapid flushing and shorter travel time through soils and rivers and also
443 lower microbial and phytoplankton activity. As a result, the zone of sporadic to isolated permafrost
444 exhibits both maximal release of soil particles and minimal uptake by in-stream processes. Further to
445 the north, shallow unfrozen peat depth and low biomass cannot supply sufficiently high suspended
446 nutrients and the particulate transport of C and N decreases. In contrast, for P, opposite gradients in
447 supply versus in stream removal may cancel out the net effect of temperature and permafrost on
448 suspended P in the river water.

449 Based on these results we can speculate on the conditions following warming and
450 permafrost thaw. On a short-term prospective (10-50 years), assuming a soil temperature rise of
451 0.15 to 0.3 degree per 10 years in WSL (Pavlov et al., 2009; Anisimov et al., 2012), the northern
452 part of the WSL (discontinuous and continuous permafrost zones) will transform into sporadic
453 and isolated permafrost zones (Anisimov and Reneva, 2006). This will lead to increase in C and
454 N concentrations in RSM, C and N particulate export yield of the watershed, and overall increase
455 in particulate versus dissolved transport of C and P. Given the contemporary maximum of C and

456 N at the permafrost thawing front, this increase may be two-fold. However, on a longer prospective
457 (50-100 years), even the continuous permafrost zone may disappear (Romanovsky et al., 2008;
458 Nadyozhina et al., 2008) and this will decrease the particulate C and N concentration in the
459 northern rivers and, consequently, their export to the coastal zone of the Kara Sea. Judging from
460 the actual difference in nutrient concentrations and fluxes among adjusting permafrost zones, this
461 decrease may be around a factor of 2 to 3. Furthermore, on the same long-term prospective, the
462 drainage of lakes and disappearance of bogs due to colonization of northern tundra by forests
463 (Anisimov et al., 2011; Anisimov and Sherstiukov, 2016; Kirpotin et al., 2008, 2009, 2011) should
464 lead to a further decrease in particulate nutrient load of WSL rivers.

465

466 **Conclusions:**

467 Relatively low bulk RSM concentration in WSL rivers stems from low runoff in this flat
468 peatland province of boreal and subarctic zone. High concentrations of C and N in the RSM of
469 WSL rivers reflect the essentially organic nature of soils across the WSL. At the isolated/sporadic
470 permafrost zone, we observed a maximum concentration of C and N in the RSM, maximal fraction
471 of particulate OC relative to total (dissolved + particulate), and maximal export fluxes. This
472 suggests the enhanced generation of C, N-rich RSM at the thawing front of permafrost, where
473 thickness of the active layer is maximal. The C and N concentrations in particulate load of WSL
474 rivers decrease with forest coverage of the watershed and increase with the proportion of lakes
475 and bogs; however, the bulk concentration of RSM did not depend on landscape parameters of
476 the watersheds. This implies generation of C, N-rich particles via coastal peat abrasion, sediment
477 resuspension, and photo- and bio-coagulation of DOM in lentic surface waters which are
478 hydrologically connected to rivers. To model a northward permafrost boundary and forest line
479 shifting with increase in air and soil temperature we used a substituting space for time scenario of
480 climate warming in the WSL that was well developed for the dissolved fraction of C and nutrients.

481 From a short-term climate warming prospective, the effect of a northward shift of permafrost
482 boundary may produce about a two-fold increase in particulate C and N concentration and **export**
483 **fluxes** in rivers of the discontinuous and continuous permafrost zones, and thus may enhance the
484 **delivery** of these nutrients by the most northern WSL rivers to the Arctic Ocean. On a long-term
485 prospective, the disappearance of permafrost in the northern part of WSL will decrease the
486 concentrations **and export** of these nutrients to their current level. The P is unlikely to be
487 significantly affected by permafrost change. Moreover, within a long-term climate warming
488 scenario, the drainage of lakes and transformation of bogs to forest may decrease nutrient
489 concentration in RSM and corresponding export flux to the Arctic Ocean.

490

491 **Acknowledgements:**

492 This work was supported by RSCF No 18-17-00237 “Mechanisms of hydrochemical runoff of the
493 Ob river...” (analyses, modeling); RFBR project № 18-35-00563\18 , Ministry of Education and
494 Science of the Russian Federation № 6.7515.2017/9.1, and by VR (the Swedish Research
495 Council) grant no. 325-2014-6898.

496

497 **References**

498

- 499 Ala-aho, P., Soulsby, C., Pokrovsky, O.S., Kirpotin, S.N., Karlsson, J., Serikova, S., Manasypov,
500 R.M., Krickov, I., Lim, A., and Tetzlaff D.: Permafrost and lakes control river isotope
501 composition across a boreal-arctic transect in the western Siberia lowland, *Environ. Res.*
502 *Lett.*, 13 (3), 034028, <https://doi.org/10.1088/1748-9326/aaa4fe>, 2018a.
- 503 Ala-Aho, P., Soulsby, C., Pokrovsky, O.S., Kirpotin, S.N., Karlsson, J., Serikova, S., Vorobyev,
504 S.N., Manasypov, R.M., Loiko, S., and Tetzlaff D.: Using stable isotopes to assess surface
505 water source dynamics and hydrological connectivity in a high-latitude wetland and
506 permafrost influenced landscape, *J. Hydrol.*, 556, 279–293,
507 <https://doi.org/10.1016/j.jhydrol.2017.11.024>, 2018b.
- 508 Anisimov, O. A., Anokhin, A., Lavrov, S. A., Malkova, G. V., Pavlov A.V., Romanovskiy, V.E.,
509 Streletskiy, D. A., Kholodov, A.,L., and Shiklomanov, N. I.: Continental multiyear
510 permafrost // *Methods of study the sequences of climate changes for nature systems*. Ed. S.M.
511 Semenov. Moscow: VNIIGMI, 2012. P. 268–328. (In Russian)
- 512 Anisimov, O.A., and Sherstiukov, A.B.: Evaluating the effect of climatic and environmental
513 factors on permafrost in Russia, *Earth`s Cryosphere*, XX (№ 2), 78–86, 2016.
- 514 Anisimov, O.A., Zhiltsova, E.L., and Reneva, S.A.: Estimation of critical levels of climate change

515 impact on natural land ecosystems of Russian territory, *Meteorology and Hydrology*, 11,
516 723-730, <https://doi.org/10.3103/S1068373911110033>, 2011.

517 Anisimov, O., and Reneva, S.: Permafrost and Changing Climate: The Russian Perspective,
518 *AMBIO*, 35(4), 169–175, <https://doi.org/10.1579/0044-7447>, 2006.

519 Attermeyer, K., Catalán, N., Einarsdottir, K., Freixa, A., Groeneveld, M., Hawkes, J. A., et al.:
520 Organic carbon processing during transport through boreal inland waters: Particles as
521 important sites. *J. Geophys. Research: Biogeosciences*, Art No123, <https://doi.org/10.1029/2018JG004500>, 2018.

522

523 Battin, T. J., Kaplan, L. A., Findlay, S., Hopkinson, C. S., Marti, E., Packman A. I., Newbold, J.
524 D., and Sabater, F.: Biophysical controls on organic carbon fluxes in fluvial networks, *Nat.*
525 *Geosci.*, 1, 95–100, <https://doi.org/10.1038/ngeo602>, 2008.

526 Blois, J. L., Williams, J. W., Fitzpatrick, M. C., Jackson, S. T., and Ferrier, S.: Space can substitute
527 for time in predicting climate-change effects on biodiversity, *PNAS*, 110 (23), 9374-9379,
528 <https://doi.org/10.1073/pnas.1220228110>, 2013.

529 Bring, A., Fedorova, I., Dibike, Y., Hinzman, L., Mård, J., Mernild, S. H., Prowse, T., Semenova,
530 O., Stuefer, S. L., and Woo, M.-K.: Arctic terrestrial hydrology: A synthesis of processes,
531 regional effects, and research challenges, *J. Geophys. Res.-Biogeo.*, 121(3), 621–649,
532 <https://doi.org/10.1002/2015JG003131>, 2016.

533 Bouwman, A. F., Bierkens, M. F. P., Griffioen, J., Hefting, M. M., Middelburg, J. J., Middelkoop,
534 H., and Slomp, C. P.: Nutrient dynamics, transfer and retention along the aquatic continuum
535 from land to ocean: towards integration of ecological and biogeochemical models,
536 *Biogeosciences* 10, 1-23, <https://doi.org/10.5194/bg-10-1-2013>, 2013.

537 Cai, Y., L. Guo, T. A. Douglas, and T. E. Whitley: Seasonal variations in nutrient concentrations
538 and speciation in the Chena River, Alaska, *J. Geophys. Res.-Biogeo.*, 113, G03035,
539 <https://doi.org/10.1029/2008JG000733>, 2008.

540 Cole, J. J., Prairie, Y. T., Caraco, N. F., McDowell, W. H., Tranvik, L. J., Striegl, R. G., Duarte, C.
541 M., Kortelainen, J. P., Downing, A., Middelburg, J. J., Melack, J.: Plumbing the Global Carbon
542 Cycle: Integrating Inland Waters into the Terrestrial Carbon Budget, *Ecosystems*, 10(1), 172–
543 185, <https://doi.org/10.1007/s10021-006-9013-8>, 2007.

544 Coppola, A.I.; Wiedemeier, D.B.; Galy, V.; Haghipour, N.; Hanke, U.M.; Nascimento, G.S.; et al.:
545 Global-scale evidence for the refractory nature of riverine black carbon. *Nature Geosciences*,
546 11, 584-588, 2018.

547 Dittmar, Th., and Kattner, G.: The biogeochemistry of the river and shelf ecosystem of the Arctic
548 Ocean: a review, *Mar. Chem.*, 83, 103-120, [https://doi.org/10.1016/S0304-4203\(03\)00105-1](https://doi.org/10.1016/S0304-4203(03)00105-1),
549 2003.

550 Dornblaser, M. M., and R. G. Striegl: Nutrient (N, P) loads and yields at multiple scales and subbasin
551 types in the Yukon River basin, Alaska, *J. Geophys. Res.-Biogeo.*, 112, G04S57,
552 <https://doi.org/10.1029/2006JG000366>, 2007.

553 Emmerton, C. A., Lesack, L. F. W., and Vincent, W. F.: Mackenzie River nutrient delivery to the
554 Arctic Ocean and effects of the Mackenzie Delta during open water conditions, *Global*
555 *Biogeochem. Cy.*, 22, GB1024, <https://doi.org/10.1029/2006GB002856>, 2008.

556 Frey, K. E., McClelland, J. W., Holmes, R. M., and Smith, L. C.: Impacts of climate warming and
557 permafrost thaw on the riverine transport of nitrogen and phosphorus to the Kara Sea, *J.*
558 *Geophys. Res.-Biogeo.*, 112, G04S58, doi:10.1029/2006JG000369, 2007a.

559 Frey, K. E., Siegel, D. I., and Smith, L.C.: Geochemistry of west Siberian streams and their potential
560 response to permafrost degradation, *Water Resour. Res.*, 43(3), W03406,
561 <https://doi.org/10.1029/2006WR004902>, 2007b.

562 Frey, K. E., and Smith, L.C.: Amplified carbon release from vast West Siberian peatlands by 2100,
563 *Geophys. Res. Lett.*, 32, L09401, <https://doi.org/10.1029/2004GL022025>, 2005.

564 Frey, K. E., and McClelland, J. W.: Impacts of permafrost degradation on arctic river

565 biogeochemistry, *Hydrol. Process.*, 23(1), 169–182, <https://doi.org/10.1002/hyp.7196>, 2009.

566 Galy, V., Peucker-Ehrenbrink, B. and Eglinton, T.: Global carbon export from the terrestrial
567 biosphere controlled by erosion, *Nature*, 521, 204–207, <http://dx.doi.org/10.1038/nature14400>,
568 2015.

569 Gareis, J. A. L., and Lesack, L. F. W.: Fluxes of particulates and nutrients during hydrologically
570 defined seasonal periods in an ice-affected great Arctic river, the Mackenzie, *Water Resour.*
571 *Res.*, 53(7), 6109–6132, <https://doi.org/10.1002/2017WR020623>, 2017.

572 Gebhardt, A. C., Gaye-Haake, C., Unger, D., Lahajnar, N., and Ittekkot V.: Recent particulate organic
573 carbon and total suspended matter fluxes from the Ob and Yenisei Rivers into the Kara Sea
574 (Siberia), *Mar. Geol.*, 207, 225–245, <https://doi.org/10.1016/j.margeo.2004.03.010>, 2004.

575 Gentsch, N., Mikutta, R., Alves, R. J. E., Barta, J., Čapek, P., Gittel, A., Hugelius, G., Kuhry, P.,
576 Lashchinskiy, N., Palmtag, J., Richter, A., Šantručková, H., Schneckner, J., Shibistova, O., Ulrich,
577 T., Wild, B., and Guggenberger, G.: Storage and transformation of organic matter fractions in
578 cryoturbated permafrost soils across the Siberian Arctic, *Biogeosciences*, 12(14), 4525-4542,
579 <http://dx.doi.org/10.5194/bg-12-4525-2015>, 2015.

580 Gladyshev, M. I., Kolmakova, O. V., Tolomeev, A. P., Anishchenko, O. V., Makhutova, O. N.,
581 Kolmakova, A. A., Kravchuk, E. S., Glushchenko, L. A., Kolmakov, V. I., and Sushchik, N.N.:
582 Differences in organic matter and bacterioplankton between sections of the largest Arctic river:
583 Mosaic or continuum?, *Limnol. Oceanogr.*, 60, 1314-1331, <https://doi.org/10.1002/lno.10097>,
584 2015.

585 Goñi, M. A., Hatten, J. A., Wheatcroft, R. A., and Borgeld, J. C.: Particulate organic matter export by
586 two contrasting small mountainous rivers from the Pacific Northwest, U.S.A., *J. Geophys. Res.-*
587 *Biogeo.*, 118, 1–23, <https://doi.org/10.1002/jgrg.20024>, 2013.

588 Gordeev, V. V., Martin, J. M., Sidorov, I. S., and Sidorova, M. V.: A reassessment of the Eurasian
589 river input of water, sediment, major elements, and nutrients to the Arctic Ocean, *Am. J. Sci.*,
590 296(6), 664–691, 1996.

591 Gordeev, V. V., and Kravchishina, M. D.: River flux of dissolved organic carbon (DOC) and
592 particulate organic carbon (POC) to the Arctic Ocean: what are the consequences of the
593 global changes?, in: *Influence of Climate Change on Changing Arctic and Sub-Arctic*
594 *Conditions*, Springer, 145-160, 2009.

595 Grosse, G., Goetz, S., McGuire, D., Romanovsky, V.E., and Schuur E. A. G.: Changing permafrost
596 in a warming world and feedbacks to the Earth system, *Environ. Res. Lett.*, 11, 040201,
597 <https://doi.org/10.1088/1748-9326/11/4/040201>, 2016.

598 Guo, L., and Macdonald, R. W.: Source and transport of terrigenous organic matter in the upper
599 Yukon River: Evidence from isotope (d13C, D14C, and d15N) composition of dissolved,
600 colloidal, and particulate phases, *Global Biogeochem. Cy.*, 20, GB2011,
601 <https://doi.org/10.1029/2005GB002593>, 2006.

602 Guo, L., Zhang, J.-Z., and Guéguen, C.: Speciation and fluxes of nutrients (N, P, Si) from the upper
603 Yukon River, *Global Biogeochem. Cy.*, 18, GB1038, <https://doi.org/10.1029/2003GB002152>,
604 2004.

605 Hilton, R. G., Galy, V., Gaillardet, J., Dellinger, M., Bryant, C., O'Regan, M., Gröcke, D.R., Coxall,
606 H., Bouchez, J., and Calmels, D.: Erosion of organic carbon in the Arctic as a geological carbon
607 dioxide sink, *Nature*, 524, 84-87, <https://doi.org/10.1038/nature14653>, 2015.

608 Hilton, R.G.: Climate regulates the erosional carbon export from the terrestrial biosphere,
609 *Geomorphology*, 277, 118-132, <https://doi.org/10.1016/j.geomorph.2016.03.028>, 2017.

610 Holmes, R. M., Peterson, B. J., Gordeev, V. V., Zhulidov, A. V., Meybeck, M., Lammers, R. B., and
611 Vorosmarty, C. J.: Flux of nutrients from Russian rivers to the Arctic Ocean: Can we establish
612 a baseline against which to judge future changes?, *Water Resour. Res.*, 36(8), 2309–2320,
613 <https://doi.org/10.1029/2000WR900099>, 2000.

- 614 Jeong, J. J., Bartsch, S., Fleckenstein, J. H., Matzner, E., Tenhunen, J. D., Lee, S. D., Park, S. K.,
615 and Park, J.-H.: Differential storm responses of dissolved and particulate organic carbon in a
616 mountainous headwater stream, investigated by high-frequency, in situ optical measurements,
617 *J. Geophys. Res.-Biogeo.*, 117(3), 1–13, <https://doi.org/10.1029/2012JG001999>, 2012.
- 618 Kirpotin, S., Polishchuk, Y., Zakharova, E., Shirokova, L., Pokrovsky, O., Kolmakova, M., and
619 Dupre, B.: One of possible mechanisms of thermokarst lakes drainage in West-Siberian North,
620 *Int. J. Environ. Stud.*, 65(5), 631–635, <https://doi:10.1080/00207230802525208>, 2008.
- 621 Kirpotin, S. N., Berezin A., Bazanov V. et al.: Western Siberia wetlands as indicator and regulator of
622 climate change on the global scale, *Internat. J. Environ. Stud.*, 66(4), 409–421, DOI:
623 [10.1080/00207230902753056](https://doi.org/10.1080/00207230902753056), 2009.
- 624 Kirpotin, S., Polishchuk, Y., Bryksina, N., Sugaipova, A., Kouraev, A., Zakharova, E., Pokrovsky,
625 O.S., Shirokova, L., Kolmakova, M., Manassypov, R., and Dupre B.: West Siberian palsa
626 peatlands: distribution, typology, hydrology, cyclic development, present-day climate-driven
627 changes and impact on CO₂ cycle, *Int. J. Environ. Stud.*, 68(5), 603–623,
628 <https://doi:10.1080/00207233.2011.593901>, 2011.
- 629 Kortelainen, P., Mattsson, T., Finér, L., Ahtiainen, M., Saukkonen, S., and Sallantausta, T.: Controls
630 on the export of C, N, P and Fe from undisturbed boreal catchments, Finland, *Aquat. Sci.*, 68(4),
631 453–468, <https://doi.org/10.1007/s00027-006-0833-6>, 2006a.
- 632 Kortelainen, P., Rantakari, M., Huttunen, J. T., Mattsson, T., Alm, J., Juutinen, S., Larmola, T.,
633 Silvola, J., and Martikainen, P. J.: Sediment respiration and lake trophic state are important
634 predictors of large CO₂ evasion from small boreal lakes, *Glob. Change Biol.*, 12, 1554–1567,
635 <https://doi.org/10.1111/j.1365-2486.2006.01167.x>, 2006b.
- 636 Kremenetski, K. V., Velichko, A. A., Borisova, O. K., MacDonald, G. M., Smith, L. C., Frey, K. E.,
637 and Orlova, L. A.: Peatlands of the West Siberian Lowlands: Current knowledge on zonation,
638 carbon content, and Late Quaternary history, *Quaternary Sci. Rev.*, 22, 703–723,
639 [https://doi.org/10.1016/S0277-3791\(02\)00196-8](https://doi.org/10.1016/S0277-3791(02)00196-8), 2003.
- 640 Kutscher, L., Mörth, C.-M., Porcelli, D., Hirst, C., Maximov, T. C., Petrov, R. E., and Andersson, P.
641 S.: Spatial variation in concentration and sources of organic carbon in the Lena River, Siberia,
642 *J. Geophys. Res.-Biogeo.*, 122, 1999–2016, <https://doi.org/10.1002/2017JG003858>, 2017.
- 643 Lal, R.: Soil erosion and the global carbon budget, *Environ. Int.*, 29, 437–450,
644 [http://dx.doi.org/10.1016/S0160-4120\(02\)00192-7](http://dx.doi.org/10.1016/S0160-4120(02)00192-7), 2003.
- 645 Lamoureux, S. F., and Lafrenière, M. J.: Seasonal fluxes and age of particulate organic carbon
646 exported from Arctic catchments impacted by localized permafrost slope disturbances, *Environ.*
647 *Res. Lett.*, 9, 045002, <https://doi:10.1088/1748-9326/9/4/045002>, 2014.
- 648 Laurion, I., and Mladenov, N.: Dissolved organic matter photolysis in Canadian Arctic thaw ponds,
649 *Environ. Res. Lett.*, 8, 035026, <https://doi:10.1088/1748-9326/8/3/035026>, 2013.
- 650 Lee, M. H., Payeur-Poirier, J. L., Park, J. H., and Matzner, E.: Variability in runoff fluxes of dissolved
651 and particulate carbon and nitrogen from two watersheds of different tree species during intense
652 storm events, *Biogeosciences*, 13(18), 5421–5432, <https://doi.org/10.5194/bg-13-5421-2016>,
653 2016.
- 654 Le Fouest, V., Babin, M., and Tremblay, J.-É.: The fate of riverine nutrients on Arctic shelves,
655 *Biogeosciences*, 10, 3661–3677, <https://doi:10.5194/bg-10-3661-2013>, 2013.
- 656 Leonov, A. B., and Chicherina, O. V.: Export of biogenic components of the riverine flux to the
657 White Sea, *Water Resour.*, 31(2), 170–192, 2004.
- 658 Li, M., Peng, C., Wang, M., Xue, W., Zhang, K., Wang, K., Shi G., and Zhu, Q.: The carbon flux of
659 global rivers: A re-evaluation of amount and spatial patterns, *Ecol. Indic.*, 80, 40–51,
660 <https://doi.org/10.1016/j.ecolind.2017.04.049>, 2017.
- 661 Lidman, F., Kohler, S. J., Morth, C.-M., and Laudon, H.: Metal transport in the boreal landscape –
662 the role of wetlands and the affinity for organic matter, *Environ. Sci. Technol.*, 48, 3783–3790,
663 <https://doi:10.1021/es4045506>, 2014.

664 Lobbes, J. M., Fitznar, H. P., and Kattner, G.: Biogeochemical characteristics of dissolved and
665 particulate organic matter in Russian rivers entering the Arctic Ocean, *Geochim. Cosmochim.*
666 *Ac.*, 64, 2973–2983, [https://doi.org/10.1016/S0016-7037\(00\)00409-9](https://doi.org/10.1016/S0016-7037(00)00409-9), 2000.

667 Loiko, S. V., Pokrovsky, O. S., Raudina, T., Lim, A., Kolesnichenko, L. G., Shirokova, L. S.,
668 Vorobyev, S. N., and Kirpotin, S. N.: Abrupt permafrost collapse enhances organic carbon, CO₂,
669 nutrient, and metal release into surface waters, *Chem. Geol.*, 471, 153–165,
670 <https://doi.org/10.1016/j.chemgeo.2017.10.002>, 2017.

671 Ludwig, W., and Probst, J. L.: Predicting the oceanic input of organic carbon by continental erosion,
672 *Global Biogeochemical Cy.*, 10(1), 23–41, <https://doi.org/10.1029/95GB02925>, 1996.

673 Manasypov, R. M., Vorobyev, S. N., Loiko, S. V., Kritzkov, I. V., Shirokova, L. S., Shevchenko, V.
674 P., Kirpotin, S. N., Kulizhsky, S. P., Kolesnichenko, L. G., Zemtsov, V. A., Sinkinov, V. V.,
675 and Pokrovsky, O. S.: Seasonal dynamics of organic carbon and metals in thermokarst lakes
676 from the discontinuous permafrost zone of western Siberia, *Biogeosciences*, 12, 3009–3028,
677 <https://doi.org/10.5194/bg-12-3009-2015>, 2015.

678 Mayer, L. M., Schick, L. L., Skoroko, K., and Boss, E.: Photodissolution of particulate organic matter
679 from sediments, *Limnol. Oceanogr.*, 51(2), 1064–1071,
680 <https://doi.org/10.4319/lo.2006.51.2.1064>, 2006.

681 McClelland, J. W., Stieglitz, M., Pan, F., Holmes, R. M., and Peterson, B. J.: Recent changes in nitrate
682 and dissolved organic carbon export from the upper Kuparuk River, North Slope, Alaska, *J.*
683 *Geophys. Res.-Biogeo.*, 112, G04S60, <http://doi.wiley.com/10.1029/2006JG000371>, 2007.

684 McClelland, J. W., Townsend-Small, A., Holmes, R. M., Pan, F., Stieglitz, M., Khosh, M., and
685 Peterson B. J.: River export of nutrients and organic matter from the North Slope of Alaska to
686 the Beaufort Sea, *Water Resour. Res.*, 50(2), 1823–1839,
687 <https://doi.org/10.1002/2013WR014722>, 2014.

688 McClelland, J. W., Holmes, R. M., Raymond, P. A., Striegl, R. G., Zhulidov, A. V., Zimov, S. A.,
689 Zimov, N., Tank, S. E., Spencer, R. G. M., Staples, R., Gurtovaya, T. Y., and Grif, C. G.:
690 Particulate organic carbon and nitrogen export from major Arctic rivers, *Global Biogeochem.*
691 *Cy.*, 30, 629–643, <https://doi.org/10.1002/2015GB005351>, 2016.

692 Meybeck, M.: C, N, P and S in rivers: from sources to global inputs, in: Wollast, R., Mackenzie, F.,
693 and Chou, L., editors, *Interaction of C, N, P, and S biogeochemical cycles and global change*,
694 *NATO ASI Series: Berlin, Heidelberg, Springer-Verlag*, 163–193, 1993.

695 Nadyozhina, E. D., Shkolnik, I. M., Pavlova, T. V., Molkentin, E. K., and Semioshina, A. A.:
696 Permafrost response to the climate warming as simulated by the regional climate model of
697 the main geophysical observatory, *Kriosfera Zemli*, XII(3), 3–11, 2008. (In Russian)

698 Pavlov, A. V., and Malkova, G. V.: Mapping of trends of the contemporary ground temperature
699 changes in the Russian north, *Kriosfera Zemli*, XIII(4), 32–39, 2009. (In Russian)

700 **Pokrovsky, O. S., Karlsson, J., Giesler, R.: Freeze-thaw cycles of Arctic thaw ponds remove colloidal**
701 **metals and generate low-molecular weight organic matter, *Biogeochemistry*, 137(3), 321–336,**
702 **2018.**

703 Pokrovsky, O. S., Manasypov, R. M., Shirokova, L. S., Loiko, S. V., Krickov, I. V., Kopysov S. G.,
704 Zemtsov, V. A., Kulizhsky, S. P., Vorobyev, S. N., and Kirpotin, S. N.: Permafrost coverage,
705 watershed area and season control of dissolved carbon and major elements in western Siberia
706 rivers, *Biogeosciences*, 12, 6301–6320, <https://doi.org/10.5194/bg-12-6301-2015>, 2015.

707 Pokrovsky, O. S., Manasypov, R. M., Loiko, S. V., Krickov, I. A., Kopysov, S. G., Kolesnichenko,
708 L. G., Vorobyev, S. N., and Kirpotin, S. N.: Trace element transport in western Siberia rivers
709 across a permafrost gradient, *Biogeosciences*, 13, 1877–1900, <https://doi.org/10.5194/bg-12-17857-2015>, 2016.

711 Pokrovsky, O. S., Schott, J., Kudryavtzev, D. I., and Dupre, B.: Basalts weathering in Central Siberia
712 under permafrost conditions, *Geochim. Cosmochim. Ac.*, 69, 5659–5680,
713 <https://doi.org/10.1016/j.gca.2005.07.018>, 2005.

- 714 Pokrovsky, O. S., Viers, J., Shirokova, L. S., Shevchenko, V. P., Filipov, A. S., and Dupré B.:
715 Dissolved, suspended, and colloidal fluxes of organic carbon, major and trace elements in
716 Severnaya Dvina River and its tributary, *Chem. Geol.*, 273, 136–149,
717 <https://doi.org/10.1016/j.chemgeo.2010.02.018>, 2010.
- 718 Polishchuk, Y. M., Bogdanov, A. N., Polischuk, V. Y., Manasypov, R. M., Shiorkova, L. S., Kirpotin,
719 S. N., and Pokrovsky, O. S.: Size-distribution, surface coverage, water, carbon and metal storage
720 of thermokarst lakes (> 0.5 ha) in permafrost zone of the Western Siberia Lowland, *Water*, 9
721 (3), 228, <https://doi.org/10.3390/w9030228>, 2017.
- 722 Polishchuk, Y. M., Bogdanov, A. N., Muratov, I. N., Polishchuk, V. Y., Lim, A., Manasypov, R. M.,
723 Shirokova, L. S., and Pokrovsky, O. S.: Minor contribution of small thaw ponds to the pools of
724 carbon and methane in the inland waters of the permafrost-affected part of western Siberian
725 Lowland, *Environ. Res. Lett.*, 13(4), 045002, <https://doi.org/10.1088/1748-9326/aab046>, 2018.
- 726 Raudina, T. V., Loiko, S. V., Lim, A. G., Krickov, I. V., Shirokova, L. S., Istignichev, G. I., Kuzmina,
727 D. M., Kulizhsky, S. P., Vorobyev, S. N., and Pokrovsky, O. S.: Dissolved organic carbon and
728 major and trace elements in peat porewater of sporadic, discontinuous, and continuous
729 permafrost zones of western Siberia, *Biogeosciences*, 14, 3561–3584,
730 <https://doi.org/10.5194/bg-14-3561-2017>, 2017.
- 731 Raudina, T.V., Loiko, S. V., Lim, A., Manasypov, R. M., Shirokova, L. S., Istigechev, G. I.,
732 Kuzmina, D. M., Kulizhsky, S. P., Vorobyev, S. N., and Pokrovsky, O. S.: Permafrost thaw and
733 climate warming may decrease the CO₂, carbon, and metal concentration in peat soil waters of
734 the Western Siberia Lowland, *Sci. Total. Environ.*, 634, 1004–1023,
735 <https://doi.org/10.1016/j.scitotenv.2018.04.059>, 2018.
- 736 Richardson, D. C., Newbold, J. D., Aufdenkampe, A. K., Taylor, P. G., and Kaplan, L. A.: Measuring
737 heterotrophic respiration rates of suspended particulate organic carbon from stream ecosystems,
738 *Limnol. Oceanogr.-Meth.*, 11(5), 247–261, <https://doi.org/10.4319/lom.2013.11.247>, 2013.
- 739 Riggsbee, J., Orr, C., Leech, D., Doyle, M., and Wetzel, R.: Suspended sediments in river ecosystems:
740 photochemical sources of dissolved organic carbon, dissolved organic nitrogen, and adsorptive
741 removal of dissolved iron, *J. Geophys. Res. Biogeosci.*, 113, G03019,
742 <https://doi.org/10.1029/2007JG000654>, 2008.
- 743 Romanovsky, V. E., Kholodov, A. L., Marchenko, S. S., Oberman, N. G., Drozdov, D. S., Malkova,
744 G. V., Moskalenko, N. G., Vasiliev, A. A., Sergeev, D. O., Zheleznyak, M. N.: Thermal State
745 and Fate of Permafrost in Russia: First Results of IPY, in: *Proceedings of the 9th International
746 Conference on Permafrost*, University of Alaska, Fairbanks, June 29 – July 3, 2008 / Kane
747 D.L., Hinkel K.M. (eds.). vol. 2, 1511–1518.
- 748 Rosgidromet, R. F.: *Doklad ob osobennostyakh klimata na territorii Rossiyskoy Federatsii za 2016
749 god*, M.: Federal'naya sluzhba po gidrometeorologii i monitoringu okruzhayushchey sredy,
750 Rosgidromet, Moscow, 2017. (In Russian)
- 751 Savenko, V. S., Pokrovskii, O. S., Dupre, B., Baturin, G. N.: *Dokl. Akad. Nauk* 398, 97–101, 2004
752 [*Dokl. Earth Sci.* 398, 938, 2004].
- 753 Serikova, S., Pokrovsky, O. S., Ala-Aho, P., Kazantsev, V., Kirpotin, S., Kopysov, S., Krickov, I.,
754 Laudon, H., Manasypov, R., Shirokova, L.S., Soulsby, C., Tetzlaff, D., Karlsson, J.: High
755 riverine CO₂ emissions at the permafrost boundary of Western Siberia. *Nature Geoscience*, in
756 press, 2018.
- 757 Sheng, Y., Smith, L. C., MacDonald, G. M., Kremenetski, K. V., Frey, K. E., Velichko, A. A., Lee,
758 M., Beilman, D. W., and Dubinin, P.: A high-resolution GIS-based inventory of the west
759 Siberian peat carbon pool, *Global Biogeochem. Cy.*, 18, GB3004,
760 <https://doi.org/10.1029/2003GB002190>, 2004.
- 761 Schlesinger, W. H., and Melack, J. M.: Transport of organic carbon in the world's rivers, *Tellus*, 33,
762 172–187, <https://doi.org/10.3402/tellusa.v33i2.10706>, 1981.

763 Schädel, C., Schuur, E. A. G., Bracho, R., Elberling, B., Knoblauch, C., Lee, H., Luo, Y., Shaver, G.
764 R., and Turetsky, M. R.: Circumpolar assessment of permafrost C quality and its vulnerability
765 over time using long-term incubation data, *Global Change Biol.*, 20, 641-652,
766 <https://doi.org/10.1111/gcb.12417>, 2014.

767 Shirokova, L. S., Pokrovsky, O. S., Kirpotin, S. N., Desmukh, C., Pokrovsky, B. G., Audry, S., Viers,
768 J.: Biogeochemistry of organic carbon, CO₂, CH₄, and trace elements in thermokarst water
769 bodies in discontinuous permafrost zones of Western Siberia, *Biogeochemistry*, 113, 573–593,
770 <https://doi.org/10.1007/s10533-012-9790-4>, 2013.

771 Stepanova, V. M., Pokrovsky, O. S., Viers, J., Mironycheva-Tokareva, N. P., Kosykh, N. P., and
772 Vishnyakova, E. K.: Elemental composition of peat profiles in western Siberia: Effect of the
773 micro-landscape, latitude position and permafrost coverage, *Appl. Geochem.*, 53, 53–70,
774 <https://doi.org/10.1016/j.apgeochem.2014.12.004>, 2015.

775 Tian, H., Yang, Q., Najjar, R., Ren, W., Friedrichs, M. A. M., Hopkinson, C. S., and Pan, S.:
776 Anthropogenic and climatic influences on carbon fluxes from Eastern North America to the
777 Atlantic ocean: a process-based modeling study, *J. Geophys. Res.-Biogeo.*, 752-772,
778 <http://dx.doi.org/10.1002/2014JG002760>, 2015.

779 Trofimova, I. E., and Balybina, A. S.: Classification of climates and climatic regionalization of the
780 West-Siberian plain, *Geography and Natural Resources*, 35(2), 114–122,
781 <https://doi.org/10.1134/S1875372814020024>, 2014.

782 Vonk, J. E., Tank, S. E., Bowden, W. B., Laurion, I., Vincent, W. F., Alekseychik, P., Amyot, M.,
783 Billet, M. F., Canário, J., Cory R. M., Deshpande, B. N., Helbig, M., Jammet, M., Karlsson, J.,
784 Larouche, J., MacMillan, G., Rautio, M., Walter Anthony, K. M., and Wickland, K. P.: Reviews
785 and syntheses: Effects of permafrost thaw on Arctic aquatic ecosystems, *Biogeosciences*,
786 12(23), 7129–7167, <https://doi.org/10.5194/bg-12-7129-2015>, 2015.

787 von Wachenfeldt, E., and Tranvik, L. J.: Sedimentation in boreal lakes - The role of flocculation of
788 allochthonous dissolved organic matter in the water column, *Ecosystems*, 11(5), 803–814,
789 <https://doi.org/10.1007/s10021-008-9162-z>, 2008.

790 Vorobyev, S. N., Pokrovsky, O. S., Serikova, S., Manasyrov, R. M., Krickov, I. V., Shirokova, L.
791 S., Lim, A., Kolesnichenko, L. G., Kirpotin, S. N., and Karlsson, J.: Permafrost boundary shift
792 in western Siberia may not modify dissolved nutrient concentrations in rivers, *Water*, 9, 985,
793 <https://doi.org/10.3390/w9120985>, 2017.

794 Wiegner, T. N., Tubal, R. L., and MacKenzie, R. A.: Bioavailability and export of dissolved organic
795 matter from a tropical river during base- and stormflow conditions, *Limnol. Oceanogr.*, 54(4),
796 1233–1242, <https://doi.org/10.4319/lo.2009.54.4.1233>, 2009.

797 **Woo, M.-K.: Permafrost Hydrology, Springer, Heidelberg Dordrecht London New York, doi**
798 **[10.1007/978-3-642-23462-0](https://doi.org/10.1007/978-3-642-23462-0), 2012.**

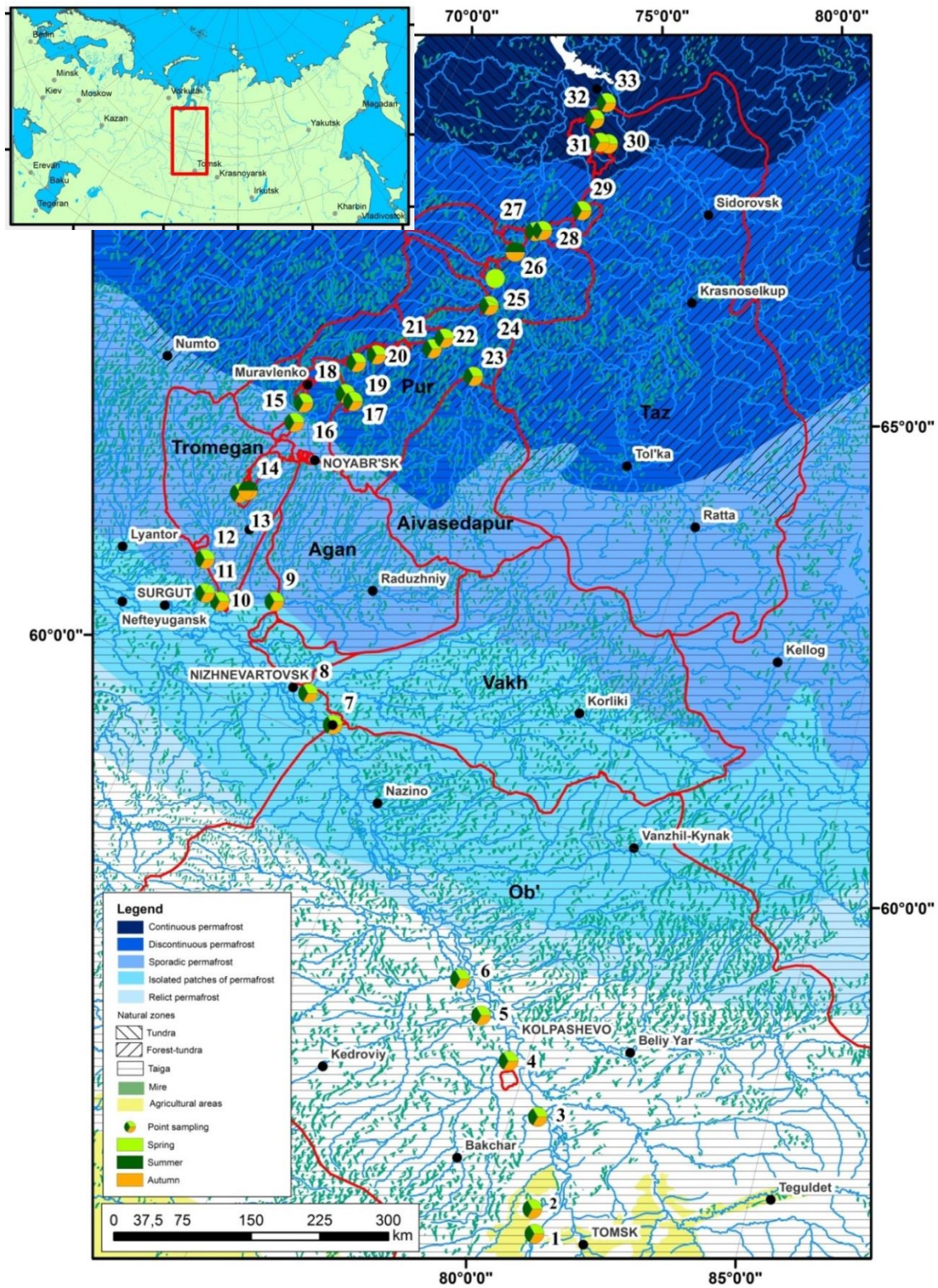
799 Wrona, F. J., Johansson M., Culp J. M., Jenkins A., Mård J., Myers-Smith, I. H., Prowse, T. D.,
800 Vincent, W. F., and Wookey, P. A.: Transitions in Arctic ecosystems: Ecological implications
801 of a changing hydrological regime, *J. Geophys. Res.-Biogeo.*, 121(3), 650–674,
802 <https://doi.org/10.1002/2015JG003133>, 2016.

803 Unger, D., Gaye-Haake, B., Neumann, K., Gebhardt, A. C., and Ittekkot, V.: Biogeochemistry of
804 suspended and sedimentary material in the Ob and Yenisei rivers and Kara Sea: amino acids
805 and amino sugars, *Cont. Shelf. Res.*, 25(4), 437-460, <https://doi.org/10.1016/j.csr.2004.09.014>,
806 2005.

807 Yang, Q., Zhang, X., Xu, X., Asrar, G. R., Smith, R. A., Shih, J. S., and Duan, S.: Spatial patterns
808 and environmental controls of particulate organic carbon in surface waters in the conterminous
809 United States, *Sci. Total. Environ.*, 554–555, 266–275,
810 <https://doi.org/10.1016/j.scitotenv.2016.02.164>, 2016.

811
812

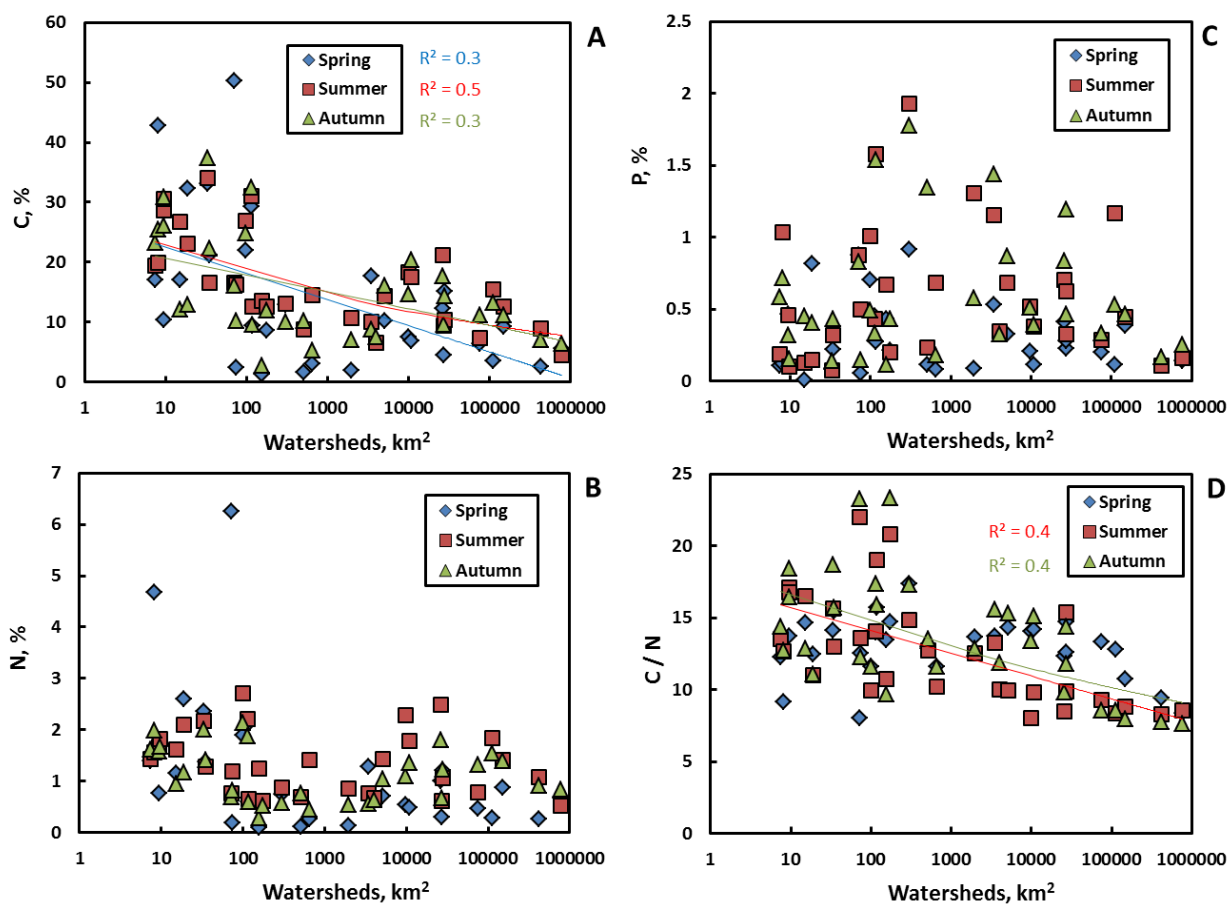
813
814



815

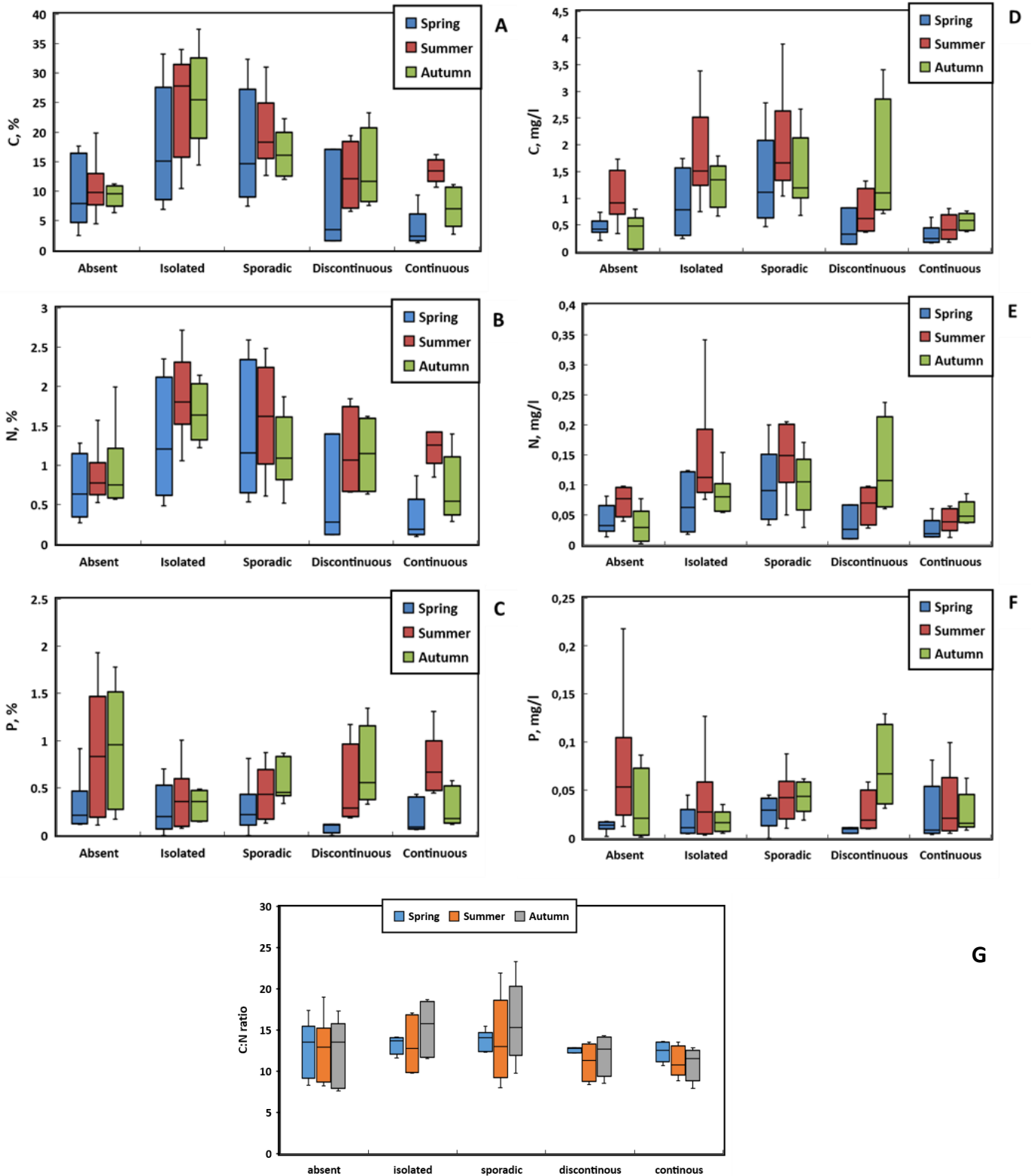
816 **Fig. 1.** Sampling sites and physio-geographical context of WSL territory investigated in this
817 work. The sampling numbers are explained in Table S1.

818
819
820



821
822
823
824
825
826
827
828
829
830

Fig. 2. Particulate ($> 0.45 \mu\text{m}$) C (A), N (B), P (C) concentration in the RMS (%) and C: N ratio (D) in RSM as a function of river watershed size. The solid lines represent a power law fitting of the data with regression coefficients shown for each season in corresponding panels. Only the curves with $R^2 > 0.3$ are depicted.

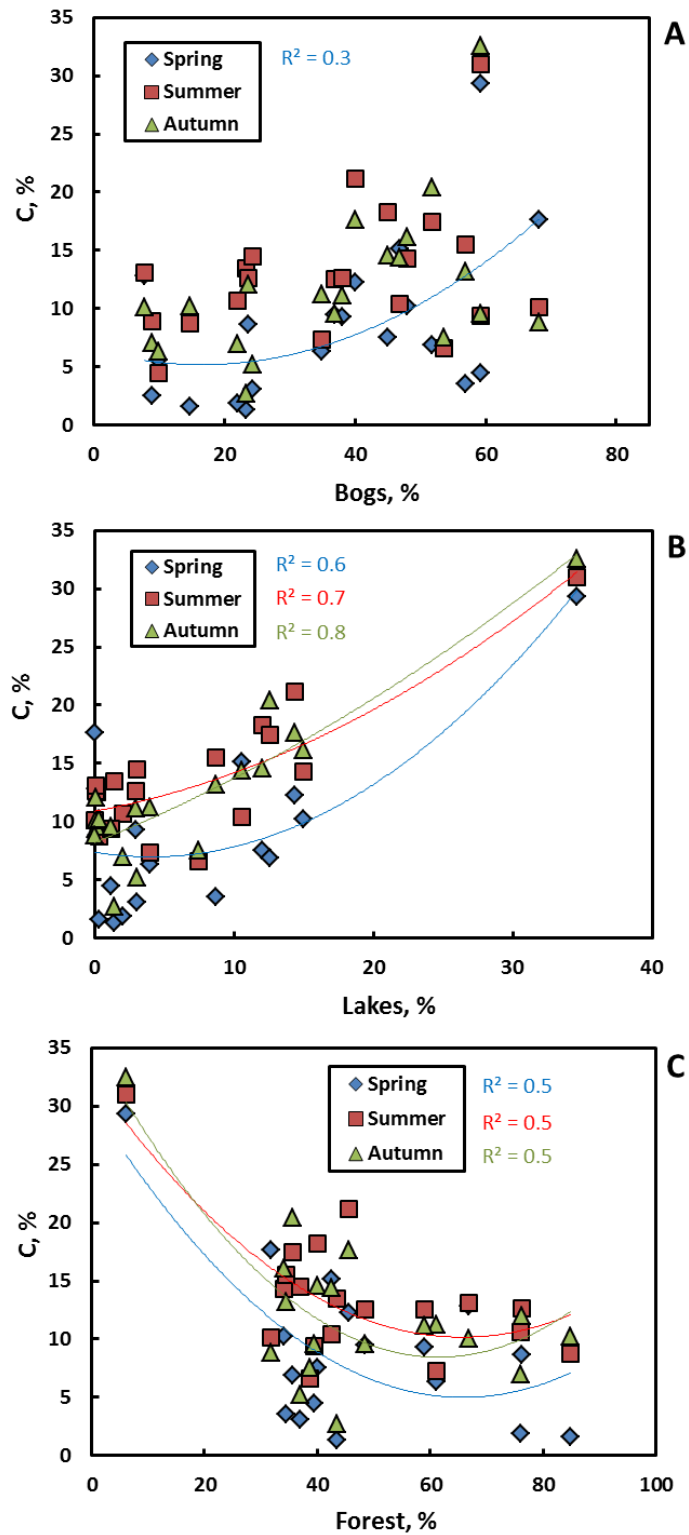


831

832

833 **Fig. 3.** Box plot of first and third quartiles (25 and 75%) of C (A), N (B) and P (C) concentration
 834 in RSM (%) in five permafrost zones over three seasons. The C, N and P concentrations in the
 835 river water are shown in panels D, E and F, respectively, and a C:N ratio is shown in G.

836



837

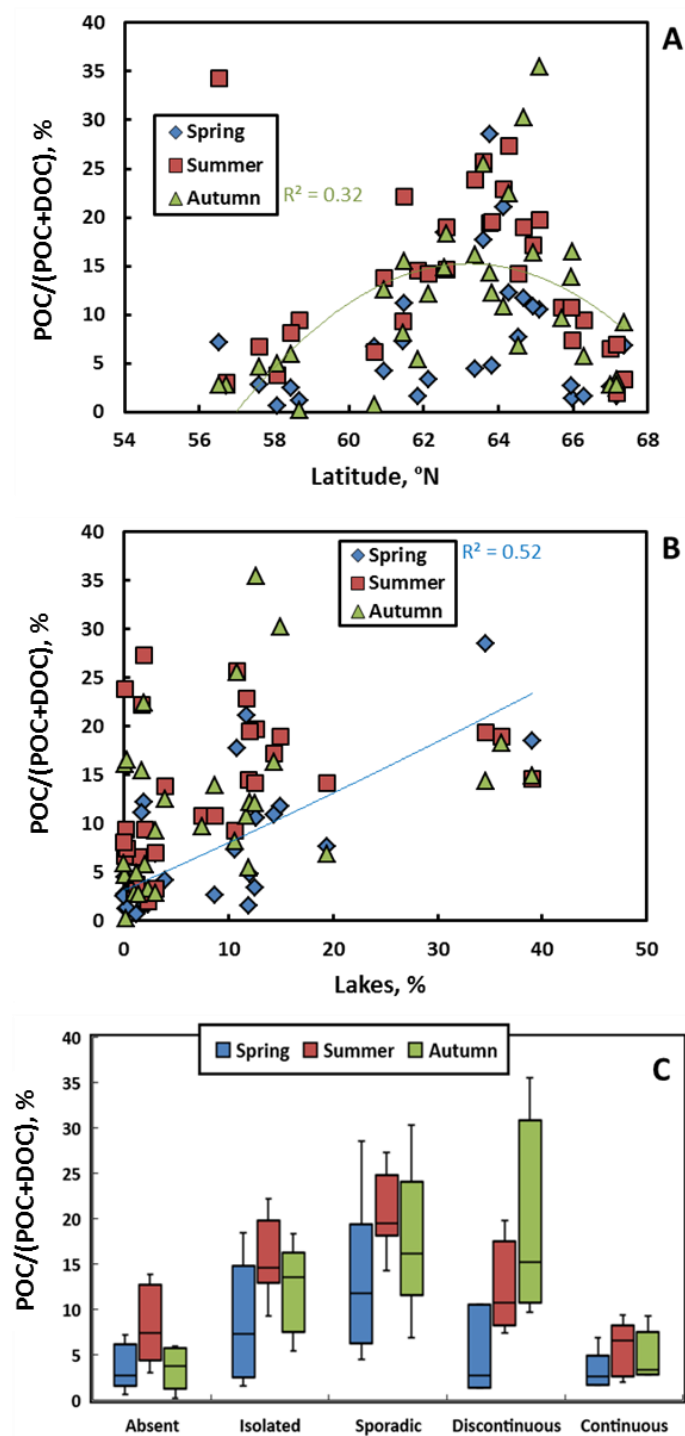
838

839 **Fig. 4.** The dependence of C concentration in RSM (%) on the coverage of watershed by bogs

840 (A), lakes (B) and forest (C). The solid lines represent 2nd degree polynomial fitting of the data

841 with regression coefficients shown for each season in corresponding panels.

842



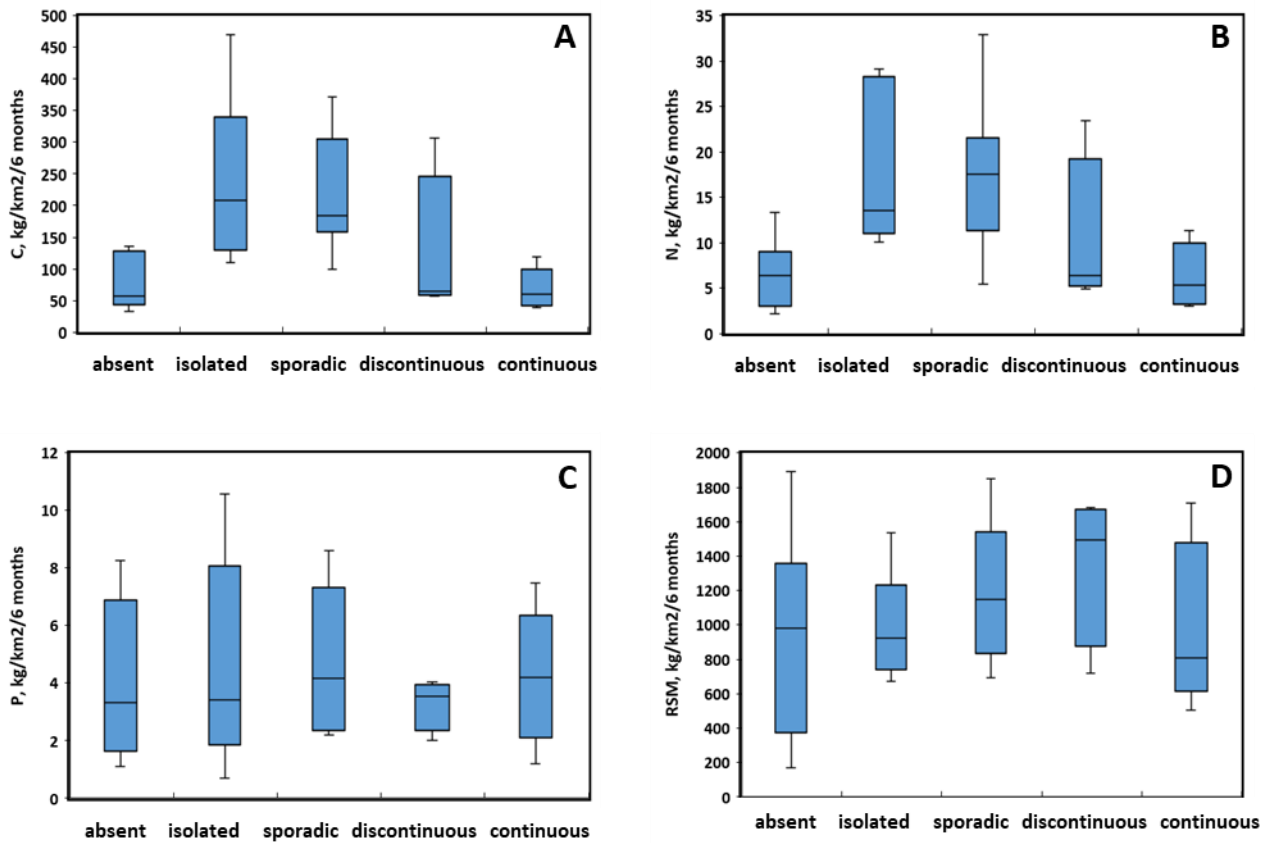
844

845

846

847 **Fig. 5.** Fraction of particulate OC of total (dissolved + particulate) form plotted as a function of
 848 latitude (A), lake fraction on the watershed (B) and a box plot of fractions for 5 permafrost zones
 849 (C). The solid lines in A and B represent 2nd degree polynomial (A, autumn) and linear (B,
 850 spring) fitting of the data with regression coefficients equal to 0.32 and 0.52, respectively.

851



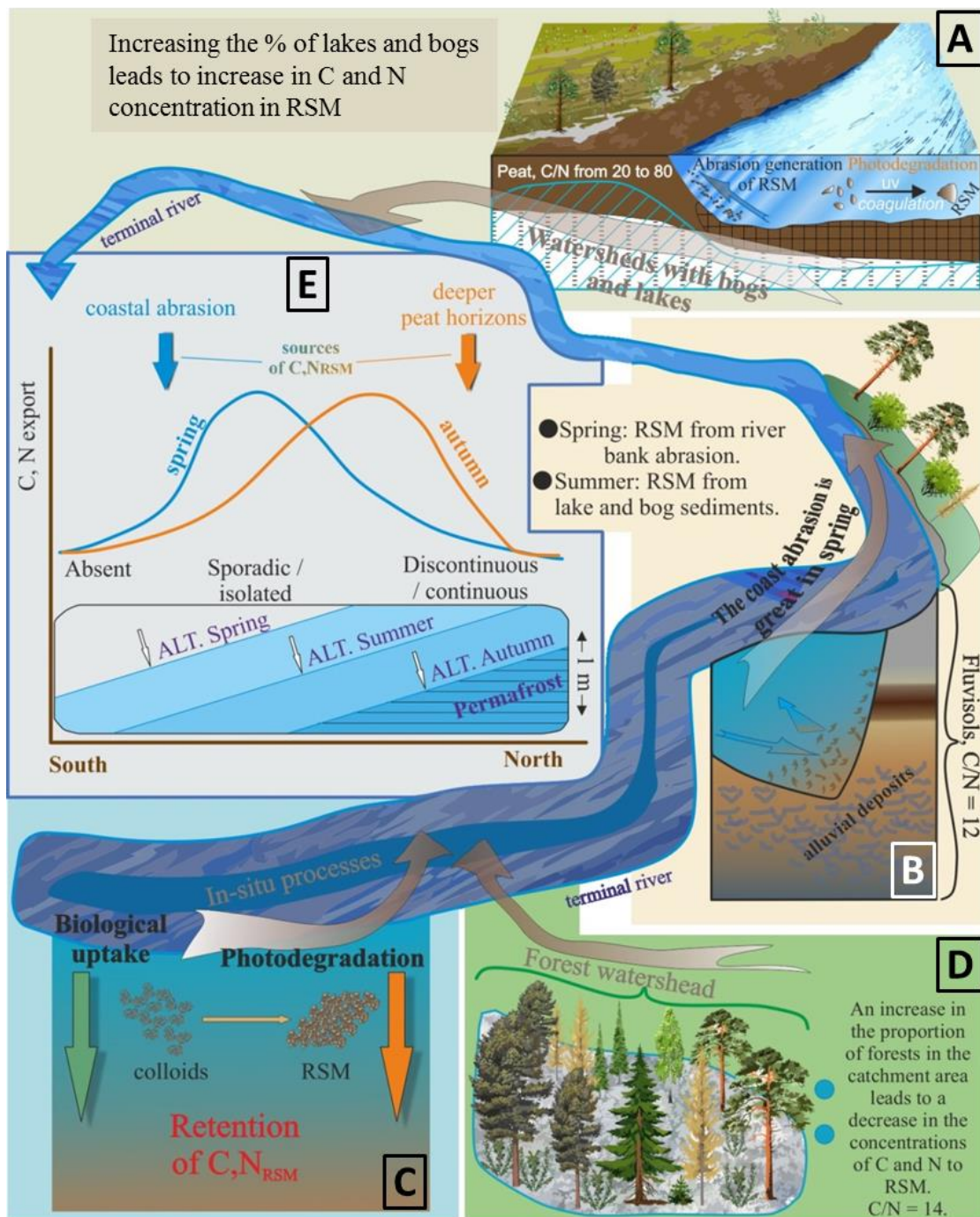
852

853

854 **Fig. 6.** Total open-water seasons fluxes of particulate C (A), N (B), P (C) and suspended
855 matter (D) in 5 permafrost-free and 4 distinct permafrost zones of WSL (box plots of 1st and
856 3rd quartiles). There is a clear maximum of C and N export at the beginning of permafrost
857 appearance, in isolated to sporadic permafrost zone.

858

859



860

861 **Fig. 7.** A cartoon of spatial and temporal partitioning of particulate nutrients in WSL rivers
 862 across the permafrost gradient. The panels **A**, **B**, **C** and **D** represent from main sources (**A**, lakes
 863 and bogs in summer and **B**, alluvial deposits in spring) and sinks (**C**, photo- and bio-degradation)
 864 and **D**, uptake by taiga forest) of particulate nutrients in WSL rivers. The panel **E** depicts the
 865 spatial gradient of C and N in RSM occurring in spring (blue line) and autumn (red line). A non
 866 steady-state physical erosion of peat soils in WSL provides the maximum of particulate nutrients
 867 within the zone of most “fragile”, actively thawing permafrost. The maximal thickness of active
 868 layer progressively moves to the north during the active season thus leading to the maximal
 869 removal of particulate C, N, and P at the thawing front.

870

871 **Table 1.** Mean (\pm SD) values of RSM, C, N, P concentration (mass %) and relative proportion
872 of suspended C and P overall total concentration for 5 permafrost zones and 3 seasons across the
873 WSL transect.

Season	Variable	Permafrost				
		Absent	Isolated	Sporadic	Discontinuous	Continuous
Spring	RSM, mg/l	6.2 \pm 4.9	4.9 \pm 1.5	7.2 \pm 3.0	7.7 \pm 2.5	10.2 \pm 4.9
	C, %	12.7 \pm 13.0	17.5 \pm 6.5	21 \pm 14	7.4 \pm 8.5	3.6 \pm 3.2
	N, %	1.4 \pm 1.5	1.3 \pm 0.8	1.8 \pm 1.8	0.6 \pm 0.7	0.3 \pm 0.3
	P, %	0.32 \pm 0.28	0.33 \pm 0.26	0.30 \pm 0.25	0.11 \pm 0.004	0.21 \pm 0.18
	% C _{RSM} of total C	3.5 \pm 2.4	8.4 \pm 6.7	13.2 \pm 7.9	4.9 \pm 5.0	3.1 \pm 2.2
	% P _{RSM} of total P	30.0 \pm 21.5	59.2 \pm 18.7	55.6 \pm 21.9	40.2 \pm 36.2	44.5 \pm 30.4
Summer	RSM, mg/l	10.0 \pm 4.6	7.5 \pm 2.9	10.2 \pm 3.7	5.8 \pm 1.5	3.6 \pm 2.5
	C, %	10.7 \pm 4.6	24.7 \pm 8.9	20.0 \pm 6.0	12.6 \pm 5.9	13.5 \pm 2.1
	N, %	0.9 \pm 0.3	1.9 \pm 0.6	1.6 \pm 0.7	1.2 \pm 0.6	1.2 \pm 0.2
	P, %	0.86 \pm 0.68	0.39 \pm 0.34	0.45 \pm 0.27	0.48 \pm 0.46	0.72 \pm 0.34
	% C _{RSM} of total C	10.7 \pm 10.1	15.6 \pm 4.4	21.0 \pm 4.2	12.2 \pm 5.3	5.6 \pm 3.0
	% P _{RSM} of P total	57.0 \pm 25.2	53.5 \pm 21.8	67.9 \pm 17.8	55.1 \pm 28.7	32.6 \pm 18.7
Autumn	RSM, mg/l	3.4 \pm 2.4	5.1 \pm 1.4	8.7 \pm 3.3	10.7 \pm 2.6	8.9 \pm 3.4
	C, %	11.0 \pm 6.0	25.7 \pm 8.0	17.4 \pm 6.5	13.6 \pm 6.9	7.3 \pm 3.5
	N, %	0.9 \pm 0.5	1.7 \pm 0.4	1.2 \pm 0.5	1.1 \pm 0.5	0.7 \pm 0.4
	P, %	0.93 \pm 0.64	0.33 \pm 0.15	0.57 \pm 0.21	0.70 \pm 0.45	0.30 \pm 0.21
	% C _{RSM} of total C	4.35 \pm 3.9	12.4 \pm 4.8	17.2 \pm 7.5	18.9 \pm 11.4	4.8 \pm 2.8
	% P _{RSM} of P total	42.8 \pm 32.7	71.9 \pm 9.9	82.8 \pm 11.4	76.9 \pm 14.0	40.8 \pm 8.6

874

875

876

877

878

879

880

SUPPLEMENTARY INFORMATION:

881 **Physico-geographical parameters of rivers, results of statistical treatment, latitudinal**
 882 **pattern of nutrient concentrations for rivers of different size, and impact of permafrost on**
 883 **nutrient concentration in rivers.**

884

885 **Table S1.** The physico-geographical characteristics of the catchments as determined by
 886 digitalizing available soil, vegetation, lithology and geocryology maps.

No on map	N	E	Description	Sarea, km ²	runoff mm.yr	bogs, %	forest, %	lakes, %	PF, %	Type of permafrost
24	65°06'48.8"	77°47'58.8"	Tydylyakha	7.5	185	49.4	37.4	12.7	49	Discontinuous
2	56°43'15.0"	83°55'35.1"	Chybyr'	8.1	44.8	19.9	28.4	1.01	0	Absent
11	61°50'28.6"	70°50'28.2"	Vachinguriyagun	9.5	192	78.7	9.4	11.9	0	Isolated
13	62°37'08.4"	74°10'15.9"	Petriyagun	9.7	192	57.2	6.7	36.1	5	Isolated
21	64°32'07.9"	76°54'21.3"	Seryareyakha	15.2	186	61.2	19.4	19.4	60	Sporadic
19	64°09'06.4"	75°22'18.1"	Apoku-Yakha	18.8	186	75.5	12.8	11.7	38	Sporadic
14	62°33'39.8"	74°00'29.5"	Pintyr'yagun	33.5	192	61	0	39	8	Isolated
16	63°36'48.2"	74°35'28.6"	Khatytayakha	34.6	194	75.3	13.2	10.8	38	Sporadic
20	64°17'31.9"	75°44'33.4"	Etu-Yakha	71.6	186	23.4	71.5	1.96	23	Sporadic
31	67°09'24.81"	78°57'31.76"	Sambotoyakha	75.0	N.D.	26.3	0.45	2.3	71	Continuous
25	65°23'34.1"	77°45'46.7"	Ponie-yakha	78.9	185	66	17.7	16.3	70	Discontinuous
10	61°29'11.1"	74°09'42.9"	Vach-Yagun	98.9	192	77.9	17.2	1.7	0	Isolated
17	63°47'04.5"	75°37'06.8"	Lymbyd'yakha	115	194	59.3	6.1	34.6	30	Sporadic
6	58°40'46.5"	84°27'56.6"	Vyalovka	117	127	37	48.4	0.19	0	Absent
30	66°59'25.84"	79°22'30.02"	Malaya Kheyaha	137	N.D.	23.4	43.4	1.4	75	Continuous
15	63°22'01.6"	74°31'53.2"	Kamgayakha	175	194	23.7	76.2	0.1	12	Sporadic
3	57°36'43.3"	83°37'02.1"	Malyi Tatosh	302	63.4	7.89	66.9	0.09	0	Absent
28	65°59'14.7"	78°32'25.2"	Malaya Khadyr-Yakha	513	278	14.8	84.9	0.3	85	Discontinuous
32	67°10'54.8"	78°51'04.5"	Nuny-Yakha	656	312	24.3	37	3.05	72	Continuous
29	66°17'10.8"	79°15'06.1"	Ngarka Khadyta-Yakha	1970	277	22	76	2	50	Continuous
5	58°26'06.9"	82°05'43.6"	Shudelka	3460	211	68.2	31.8	0.0	0	Absent
26	65°41'51.1"	78°01'05.0"	Yamsovey	4030	309	53.7	38.7	7.5	54	Discontinuous
22	64°40'14.0"	77°05'27.2"	Purpe	5110	309	48	34	15	48	Sporadic
18	63°49'54.2"	75°22'47.1"	Pyakupur	9881	324	45	40	12	34	Sporadic
12	62°07'50.0"	73°44'05.6"	Tromyegan	10770	263	51.9	35.6	12.6	10	Isolated
23	64°55'55.1"	77°56'08.2 "	Aivasedapur	26100	309	40.1	45.5	14.4	20	Sporadic
9	58°04'20.8"	82°49'19.7"	Chaya	27622	291	46.9	42.5	10.6	5	Absent
4	61°26'13.6"	74°47'39.7"	Agan	27600	291	46.9	42.5	10.6	5	Isolated
8	60°55'41.0"	76°53'49.3"	Vakh	75090	298	35	61	4	5	Absent
27	65°57'05.5"	78°18'59.1"	Pur	112000	298	56.9	34.4	8.7	34	Discontinuous
33	67°22'13.28"	79°00'25.9"	Taz	150000	330	38	59	3	59	Continuous
1	59°03'45.5"	80°52'08.9"	Ob'	520000	N.D.	9	N.D.	N.D.	0	Absent
7	60°40'28.8"	77°31'29.4"	Ob'	773200	216	10	N.D.	N.D.	0	Absent

887 PF is for permafrost, % of watershed coverage. Full dataset of measured parameters is available at the Research gate
 888 (DOI:10.13140/RG.2.2.36650.93121); <https://www.researchgate.net/publication/325334684>.

889

890 **Table S2.** Correlation matrix of watershed physico-geographical parameters and particulate
 891 nutrient concentration. All rivers, June and August and September. Marked (bold and red)
 892 Pearson correlations $R > 0.28$ are significant at $p < 0.09$. Lat and Permaf. are for Latitude ($^{\circ}$ N)
 893 and permafrost coverage of the watershed, %. The runoff is in mm y^{-1} and bogs, forest and lakes
 894 represent the % coverage in the watershed

895

Spring 2016								
permafrost-free (N=8)		Lat	S, km ²	runoff	Bogs	Forest	Lakes	Permaf
	RSM, mg/l	0.87	0.91	0.67	0.12	0.62	0.79	-
	N, %	-0.61	-0.38	-0.44	-0.33	-0.60	-0.12	-
	C, %	-0.65	-0.47	-0.46	-0.34	-0.59	-0.23	-
	% C _{RSM} of total C	0.44	0.49	0.53	-0.38	0.36	0.58	-
	P	-0.19	-0.37	-0.18	-0.28	0.51	-0.49	-
	% P _{RSM} of P total	0.95	0.88	0.87	0.03	0.62	0.80	-
permafrost-bearing (N=24)	RSM, mg/l	0.55	-0.004	0.11	-0.39	0.19	-0.24	0.52
	N, %	-0.55	-0.16	-0.53	0.66	-0.69	0.72	-0.50
	C, %	-0.55	-0.21	-0.56	0.66	-0.72	0.78	-0.48
	% C _{RSM} of total C	-0.29	-0.16	-0.38	0.47	-0.61	0.75	-0.25
	P	-0.28	0.05	-0.13	0.33	-0.24	-0.10	-0.36
% P _{RSM} of P total	-0.24	-0.15	-0.44	0.34	-0.51	0.40	-0.27	
Summer 2016								
permafrost-free (N=8)	RSM, mg/l	0.76	0.42	0.67	0.38	0.18	0.34	-
	N, %	-0.55	-0.27	-0.43	-0.53	-0.39	-0.01	-
	C, %	-0.81	-0.66	-0.76	-0.54	-0.41	-0.43	-
	% C _{RSM} of total C	0.92	0.63	0.87	0.05	0.57	0.56	-
	P	-0.54	-0.81	-0.57	-0.44	0.21	-0.82	-
% P _{RSM} of P total	0.53	0.01	0.52	0.20	0.41	-0.15	-	
permafrost-bearing (N=24)	RSM, mg/l	-0.43	-0.38	-0.40	0.55	-0.30	-0.05	-0.28
	N, %	-0.35	0.06	-0.10	0.60	-0.67	0.50	-0.41
	C, %	-0.53	-0.24	-0.61	0.63	-0.78	0.76	-0.52
	% C _{RSM} of total C	-0.53	-0.45	-0.58	0.38	-0.26	0.20	-0.50
	P	0.29	0.24	0.34	-0.24	0.32	-0.46	0.05
% P _{RSM} of P total	-0.27	-0.28	-0.16	0.35	-0.21	-0.17	-0.22	
Autumn 2016								
permafrost-free (N=8)	RSM, mg/l	0.29	0.52	0.45	0.41	-0.01	0.40	-
	N, %	-0.13	0.20	-0.09	-0.39	-0.31	0.45	-
	C, %	-0.51	-0.20	-0.43	-0.44	-0.47	0.08	-
	% C _{RSM} of total C	0.74	0.88	0.78	0.12	0.37	0.83	-
	P	-0.45	-0.74	-0.46	0.01	-0.12	-0.88	-
	% P _{RSM} of P total	0.29	0.52	0.45	0.41	-0.01	0.40	-
permafrost-bearing (N=24)	RSM, mg/l	0.51	-0.12	0.09	-0.17	0.19	-0.34	0.61
	N, %	-0.55	0.17	-0.23	0.70	-0.64	0.60	-0.61
	C, %	-0.69	-0.18	-0.50	0.60	-0.66	0.78	-0.67
	% C _{RSM} of total C	-0.16	-0.13	-0.21	0.12	-0.02	0.17	-0.12
	P	0.17	0.05	0.28	-0.36	0.60	-0.36	0.26
% P _{RSM} of P total	-0.42	-0.23	-0.43	0.37	-0.29	0.32	-0.28	

All seasons								
permafrost-free (N=24)	RSM, mg/l	0.41	0.35	0.37	0.14	0.36	0.27	-
	N, %	-0.47	-0.25	-0.39	-0.53	-0.42	-0.03	-
	C, %	-0.61	-0.42	-0.51	-0.52	-0.55	-0.19	-
	% C _{RSM} of total C	0.62	0.58	0.64	-0.01	0.50	0.54	-
	P	-0.25	-0.50	-0.20	0.24	-0.26	-0.56	-
	% P _{RSM} of P total	0.48	0.32	0.56	0.33	0.31	0.20	-
permafrost-bearing (N=70)	RSM, mg/l	0.18	-0.18	-0.09	0.03	0.01	-0.20	0.26
	N, %	-0.44	0.01	-0.27	0.60	-0.62	0.55	-0.47
	C, %	-0.57	-0.21	-0.54	0.60	-0.69	0.74	-0.54
	% C _{RSM} of total C	-0.29	-0.23	-0.36	0.29	-0.25	0.32	-0.26
	P	0.12	0.11	0.19	-0.15	0.28	-0.32	0.03
	% P _{RSM} of P total	-0.28	-0.21	-0.32	0.33	-0.31	0.15	-0.24

896

897 Correlation matrix of watershed physico-geographical parameters and particulate nutrient
898 concentration. All rivers, all seasons, $p < 0.05$

		Latitude	S, km ²	runoff	Bogs	Forest	Lakes	Permaf
permafrost-free (N=24)	RSM. mg/l	0.41	0.35	0.37	0.14	0.36	0.27	-
	N. %	-0.47	-0.25	-0.39	-0.53	-0.42	-0.03	-
	C. %	-0.61	-0.42	-0.51	-0.52	-0.55	-0.19	-
	% C _{RSM} of total C	0.62	0.58	0.64	-0.01	0.50	0.54	-
	P	-0.25	-0.50	-0.20	0.24	-0.26	-0.56	-
	% P _{RSM} of P total	0.48	0.32	0.56	0.33	0.31	0.20	-
permafrost-bearing (N=70)	RSM. mg/l	0.18	-0.18	-0.09	0.03	0.01	-0.20	0.26
	N. %	-0.44	0.01	-0.27	0.60	-0.62	0.55	-0.47
	C. %	-0.57	-0.21	-0.54	0.60	-0.69	0.74	-0.54
	% C _{RSM} of total C	-0.29	-0.23	-0.36	0.29	-0.25	0.32	-0.26
	P	0.12	0.11	0.19	-0.15	0.28	-0.32	0.03
	% P _{RSM} of P total	-0.28	-0.21	-0.32	0.33	-0.31	0.15	-0.24

899

900

901

902

903

904

905

906

907

908

909

910

911

912

913 **Table S3.** Compilation of statistical parameters for the differences in RSM, C, N and P
 914 concentration (N=32) among watersheds of different size (<100, 100-1000, 1000-50000, >50000
 915 km²)

916 **Table S3-A:** Non-parametric H-criterion Kruskal Wallis for un-paired data, at p < 0.05

Season	Variable	H	p-level
Spring	RSM	-	-
	C	10.98	0.0118
	N	10.55	0.0145
	P	-	-
Summer	RSM	-	-
	C	15,74	0.0013
	N	-	-
	P	-	-
Autumn	RSM	-	-
	C	11,02	0,0116
	N	10,72	0,0133
	P	-	-

917

918 **Table S3-B:** Impact of the watershed area ($S_{\text{watershed}}$) on RSM and nutrient concentration. Mann-
 919 Whitney U test, statistically significant (at p < 0.05) differences are in bold red. (N=32)

Water shed, km ²	Variable									
		Spring			Summer			Autumn		
		U	Z	p-level	U	Z	p-level	U	Z	p-level
<100/1000	RSM, mg/l	20.0	-	0.1571	28.0	0.906	0.365	37.00	0.091	0.928
	C, %	11.0	2.294	0.0218	10.0	2.537	0.011	12.00	2.355	0.019
	N, %	10.0	2.391	0.0168	16.0	1.992	0.046	9.00	2.626	0.009
	P, %	25.0	-	0.525	23.0	-1.359	0.174	32.00	-0.543	0.587
100-1000/1000-50000	RSM, mg/l	26.0	0.174	0.862	21.0	-1.059	0.290	22.50	-0.900	0.368
	C, %	23.0	-	0.603	27.0	0.423	0.672	25.00	-0.635	0.525
	N, %	22.0	-	0.524	24.0	-0.741	0.459	17.00	-1.481	0.138
	P, %	26.0	0.174	0.862	31.0	0.0000	1.000	29.00	-0.212	0.832
1000-50000/>50000	RSM, mg/l	8.00	-	0.092	21.0	0.133	0.894	22.50	-0.900	0.368
	C, %	10.0	1.391	0.164	13.0	1.200	0.230	25.00	-0.635	0.525
	N, %	13.00	0.952	0.341	20.00	0.267	0.790	17.00	-1.482	0.138
	P, %	13.00	0.952	0.341	11.00	1.4667	0.1425	29.00	-0.212	0.832

920

921

922

923 **Table S3-C.** Non-parametric H-criterion Kruskal Wallis for un-paired data, at $p < 0.05$. Difference
 924 between parameters depending on type of permafrost (Absent, Isolated, Sporadic, Discontinuous,
 925 Continuous)

Season	Variable	H	p-level
Spring	RSM	-	-
	C	12.07	0.017
	N	10.59	0.031
	P	-	-
Summer	RSM	15.81	0.0033
	C	14.77	0.0052
	N	11.33	0.0230
	P	-	-
Autumn	RSM	18.28	0.0004
	C	10.68	0.014
	N	7.86	0.049
	P	-	-

926

927 **Table S3-D.** Mann-Whitney U test of the difference in nutrient concentration between two
 928 adjacent permafrost zones. Statistically significant (at $p < 0.05$) differences are in bold red.
 929 (N=32)

Permafrost/	Variable	Spring			Summer			Autumn		
		U	Z	p-level	U	Z	p-level	U	Z	p-level
Permafrost/ Absent	RSM, mg/l	61.0	-1.266	0.205	63.5	1.414	0.157	22.0	-3.22	0.001
	C, %	82.0	-0.281	0.778	33.0	-2.74	0.006	48.0	-2.09	0.037
	N, %	81.0	-0.328	0.743	34.0	-2.70	0.007	68.0	-1.22	0.223
	P, %	70.0	0.683	0.495	71.0	1.088	0.277	61.0	1.52	0.128
Absent/ Isolated	RSM, mg/l	19.0	-0.073	0.942	14.5	1.162	0.245	14.0	-1.226	0.220
	C, %	11.0	-1.244	0.213	4.0	-2.52	0.012	3.0	-2.647	0.008
	N, %	11.0	-1.244	0.213	2.0	-2.77	0.006	5.0	-2.388	0.017
	P, %	20.0	0.452	0.651	13.0	1.356	0.175	11.0	1.614	0.107
Sporadic/ Discontinuous	RSM, mg/l	13.0	0.0	1.0	2.0	2.39	0.017	16.0	-1.221	0.222
	C, %	5.0	1.479	0.139	7.0	1.620	0.105	28.0	0.053	0.958
	N, %	6.0	1.294	0.196	10.0	1.157	0.247	23.0	-0.478	0.633
	P, %	6.5	1.697	0.090	18.0	-0.077	0.939	18.0	-1.009	0.313
Discontinuous/ Continuous	RSM, mg/l	6.0	-0.298	0.766	4.0	1.347	0.178	6.0	0.857	0.391
	C, %	5.0	0.596	0.551	9.0	-0.122	0.903	3.0	1.592	0.111
	N, %	5.0	0.596	0.551	10.0	0.122	0.903	4.0	1.347	0.178
	P, %	9.0	-0.122	0.903	4.0	-1.347	0.178	3.0	1.592	0.111

930

931 **Table S3-E.** Mann-Whitney U test for the impact of bog coverage of the watershed on RSM and
 932 nutrient concentration, for < 10% and > 10% of lake coverage. Statistically significant (at p <
 933 0.05) differences are in bold red. (N=30)

934

Variable	Spring			Summer			Autumn		
	U	Z	p-level	U	Z	p-level	U	Z	p-level
RSM, mg/l	90.0	0.0	1.0	100.5	-0.863	0.388	103.5	-0.748	0.454
C, %	44.0	-2.22	0.026	30.0	-3.568	0.0004	24.0	-3.799	0.0001
N, %	44.0	-2.22	0.026	32.0	-3.492	0.0005	43.0	-3.070	0.0021
P, %	76.0	-0.386	0.700	63.0	2.302	0.0213	104.0	0.729	0.4660

935

936

937 **Table S3-F.** Mann-Whitney U test for the impact of bog coverage of the watershed on RSM and
 938 nutrient concentration, for < 50% and > 50% of bog coverage. Statistically significant (at p <
 939 0.05) differences are in bold red (N=30)

940

Variable	Spring			Summer			Autumn		
	U	Z	p-level	U	Z	p-level	U	Z	p-level
RSM, mg/l	83.0	0.904	0.366	93.5	-1.132	0.258	119.0	-0.153	0.878
C, %	58.0	-1.980	0.048	63.0	-2.30	0.021	71.0	-1.995	0.046
N, %	62.0	-1.808	0.0707	70.0	-2.03	0.042	68.0	-2.110	0.035
P, %	77.0	-0.967	0.334	94.0	1.11	0.266	97.0	0.998	0.318

941

942

943 **Table S3-G.** Mann-Whitney U test for the impact of bog coverage of the watershed on RSM and
 944 nutrient concentration, for < 30% and > 30% of forest coverage. Statistically significant (at p <
 945 0.05) differences are in bold red. (N=30)

946

Variable	Spring			Summer			Autumn		
	U	Z	p-level	U	Z	p-level	U	Z	p-level
RSM, mg/l	76.0	-0.443	0.658	87.0	0.550	0.582	68.0	-1.386	0.166
C, %	31.0	2.656	0.0079	11.0	3.893	0.0001	29.0	3.102	0.0019
N, %	33.0	2.558	0.0105	38.0	2.705	0.007	31.0	3.014	0.0026
P, %	80.0	0.0258	0.9795	57.0	-1.869	0.062	46.0	-2.354	0.0186

947

948

949

950

951

952

953

954

955

956

957

958

959 **Table S4.** Mean C:N values in soils and lake sediments of WSL river watersheds.

960

Site	Mean \pm SD
Cryosols in Tazovsky, south tundra, mineral soils	14.0 \pm 7.0
Cryic Histosols, polygonal southern tundra in Tazovsky, (CkTz15)	24.3 \pm 5.7
Cryic Histosols, polygonal southern tundra in Tazovsky (CkTz14-2)	28.4 \pm 10.7
Cryic Histosols, depression over permafrost, southern tundra (CkTz14-3)	39.5 \pm 20.1
Soil of recently drained lakes, south tundra, Tazovsky, 2016	22.4 \pm 3.0
Sediments of thermokarst lake in Tazovsky, continuous permafrost	27.3 \pm 8.1
Fluvisols in Taz River flood zone, south tundra, continuous permafrost	14.9 \pm 2.2
Cryic Histosols, frozen mound in Pangody, forest-tundra (CkP15)	50.0 \pm 16.3
Thermokarst lake sediment Pangody, August 2015	27.7 \pm 7.3
Cryic Histosols, frozen mound in northern taiga Khanymey (X17-9)	43.6 \pm 19.6
Cryic Histosols, frozen mound in northern taiga Khanymey (X14-4)	57.1 \pm 16.8
Albic Alisol, light color soil, Khanymey, northern taiga Khanymey	13.0 \pm 6.4
Thermokarst lake sediment Khanymey, August 2015	24.0 \pm 3.0
Histosols, bog, ridge, northern taiga, Kogalym , sporadic perm. (Kg16-1)	65.4 \pm 21.1
Thermokarst lake sediment Kogalym, August 2015	26.8 \pm 2.5
Histosols, bog, depression, middle taiga (Stepanova et al., 2015)	36.3 \pm 18.8
Histosols, bog, ridge, middle taiga (Stepanova et al., 2015)	79.4 \pm 25.5
Fluvisols in floodzone of the Ob River, southern taiga, Kaibasovo, 2017	11.0 \pm 1.4

961

962

963

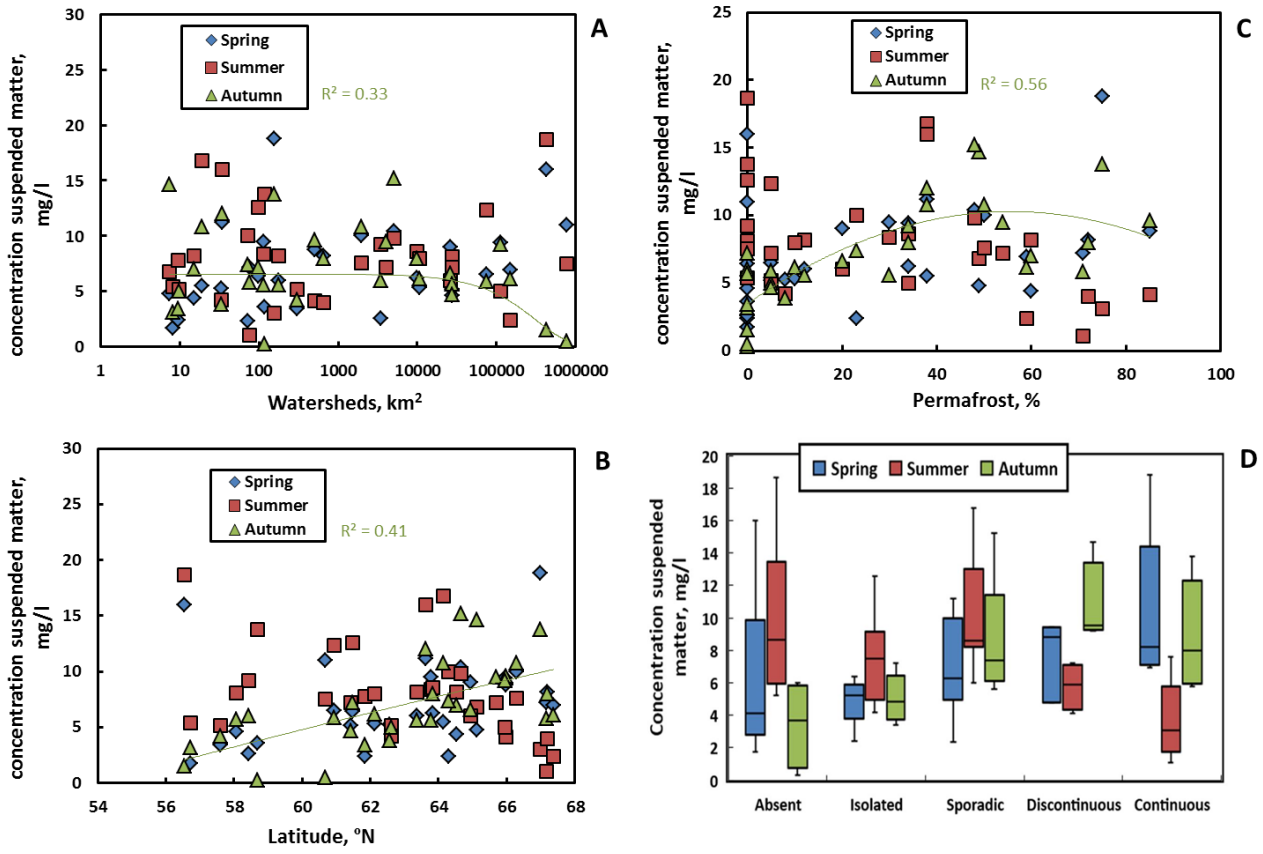
964

965

966

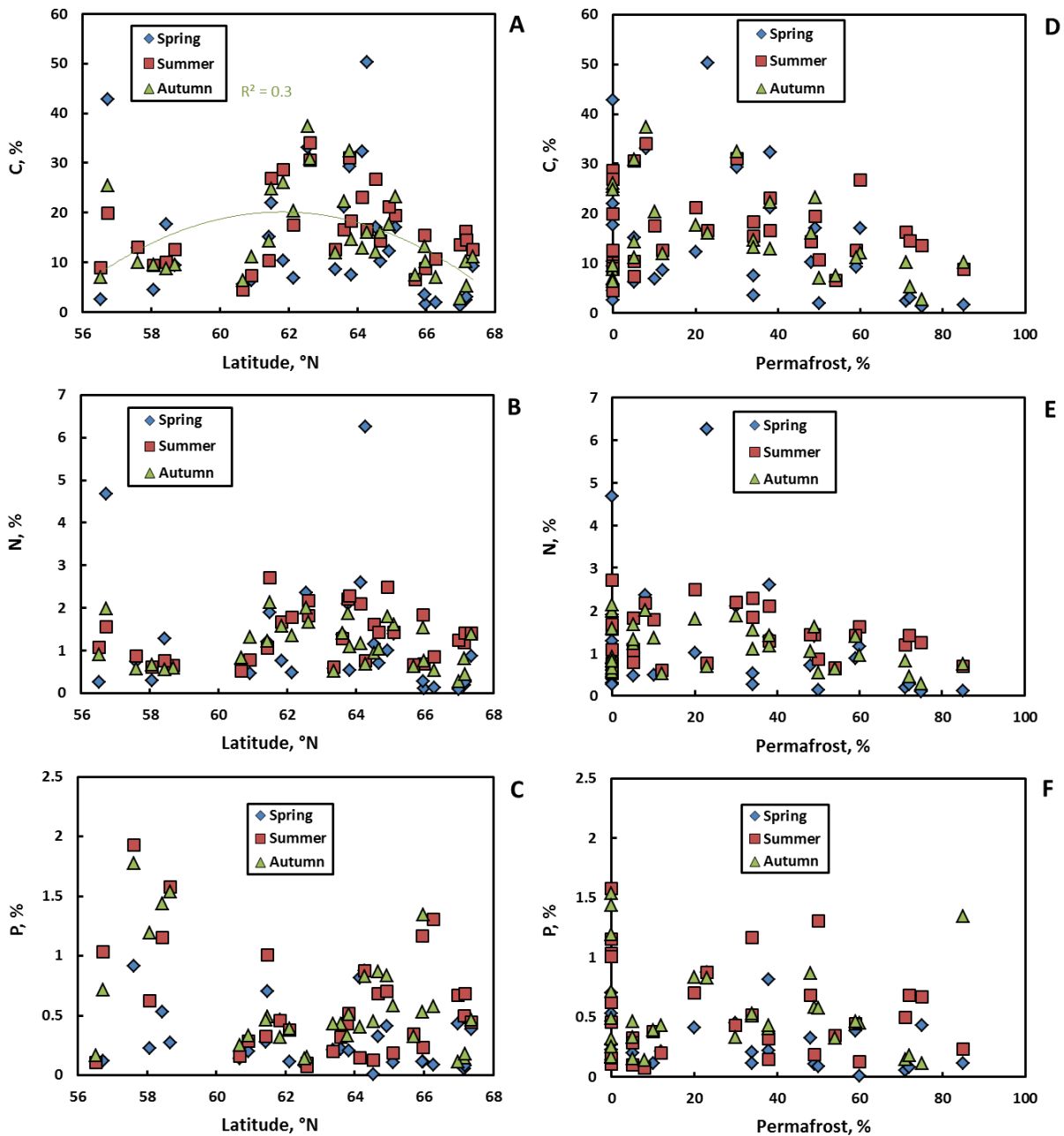
967

968



969
 970
 971
 972
 973
 974

Fig. S1. Effect of watershed size (A), latitude (B), permafrost coverage (C) and box-plot of permafrost type (D) on RSM concentration in WSL rivers.

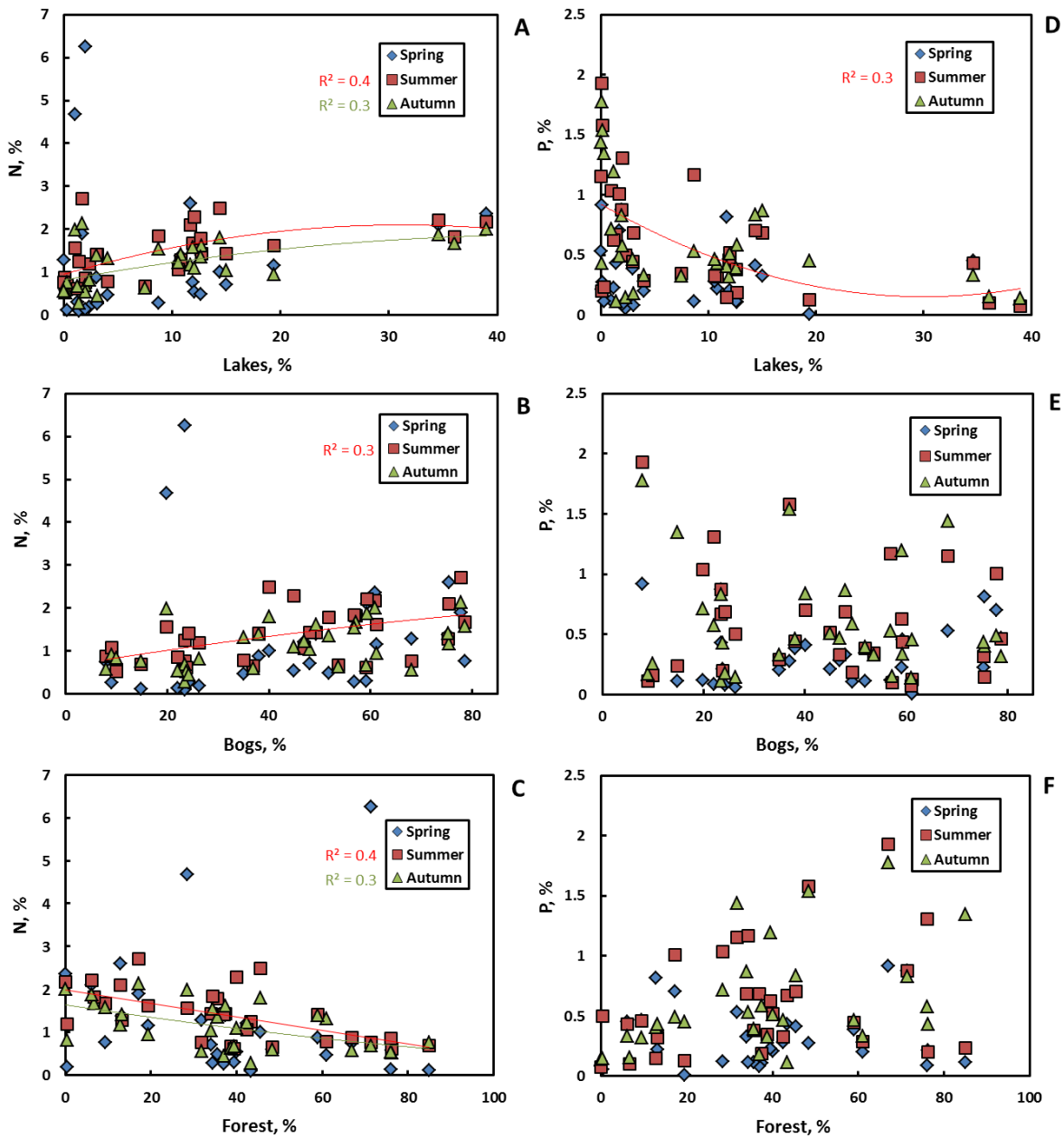


975

976

977 **Fig. S2.** Latitudinal dependences of C (A), N (B) and P (C) concentrations in RSM. A maximum
 978 in C concentrations is observed at 62-64°N, of the isolated to sporadic permafrost zone, where
 979 the maximal thawing of permafrost occurs (A). C (D), N (E) and P (F) concentration in RMS of
 980 WSL rivers as a function of permafrost coverage of the watershed. There is a general decrease of
 981 C and N concentration with an increase in permafrost coverage, consistent with maximal
 982 nutrient concentration at the beginning of permafrost appearance.

983



984

985

986 **Fig. S3.** N (A-C) and P (D-F) concentration in RSM (mass %) of WSL rivers as a function of
 987 lakes (A, D), bogs (B, E) and forest (C, F) coverage of the watershed during different seasons.

988

989

990

991

992

993

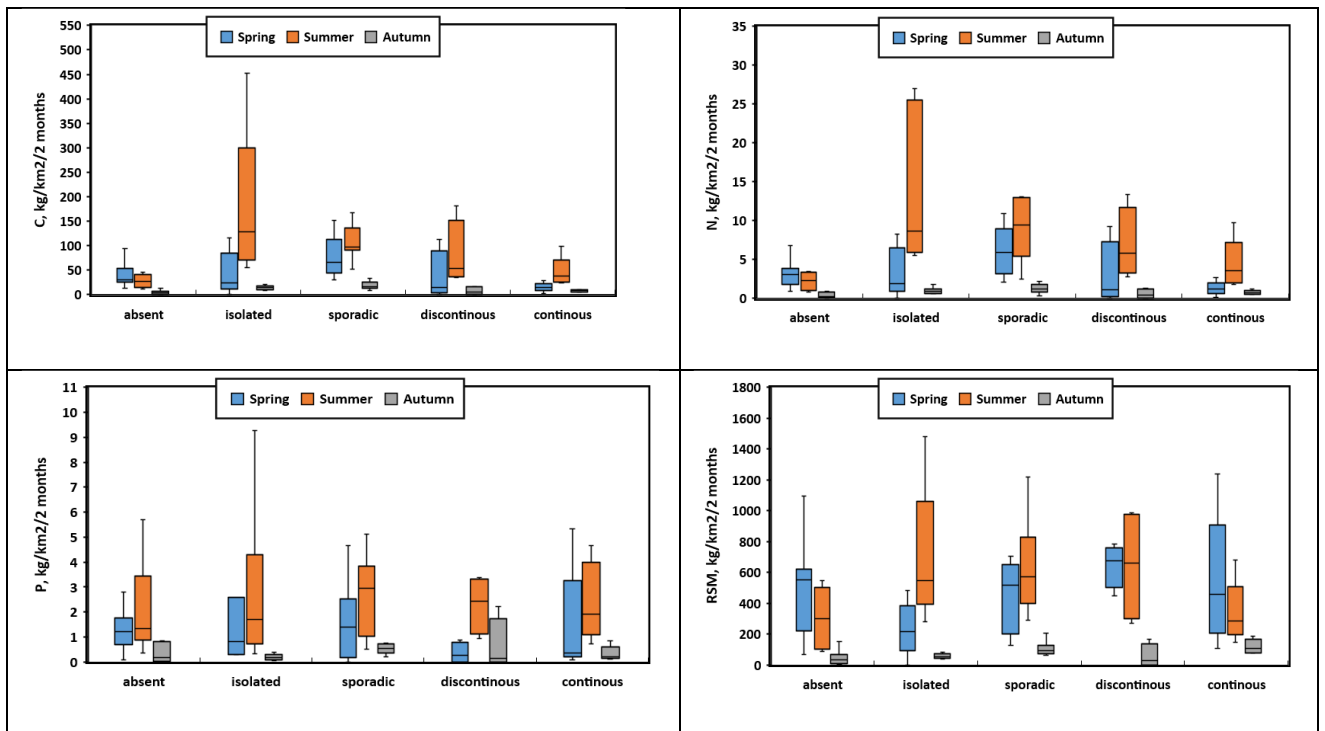
994

995

996

997

998

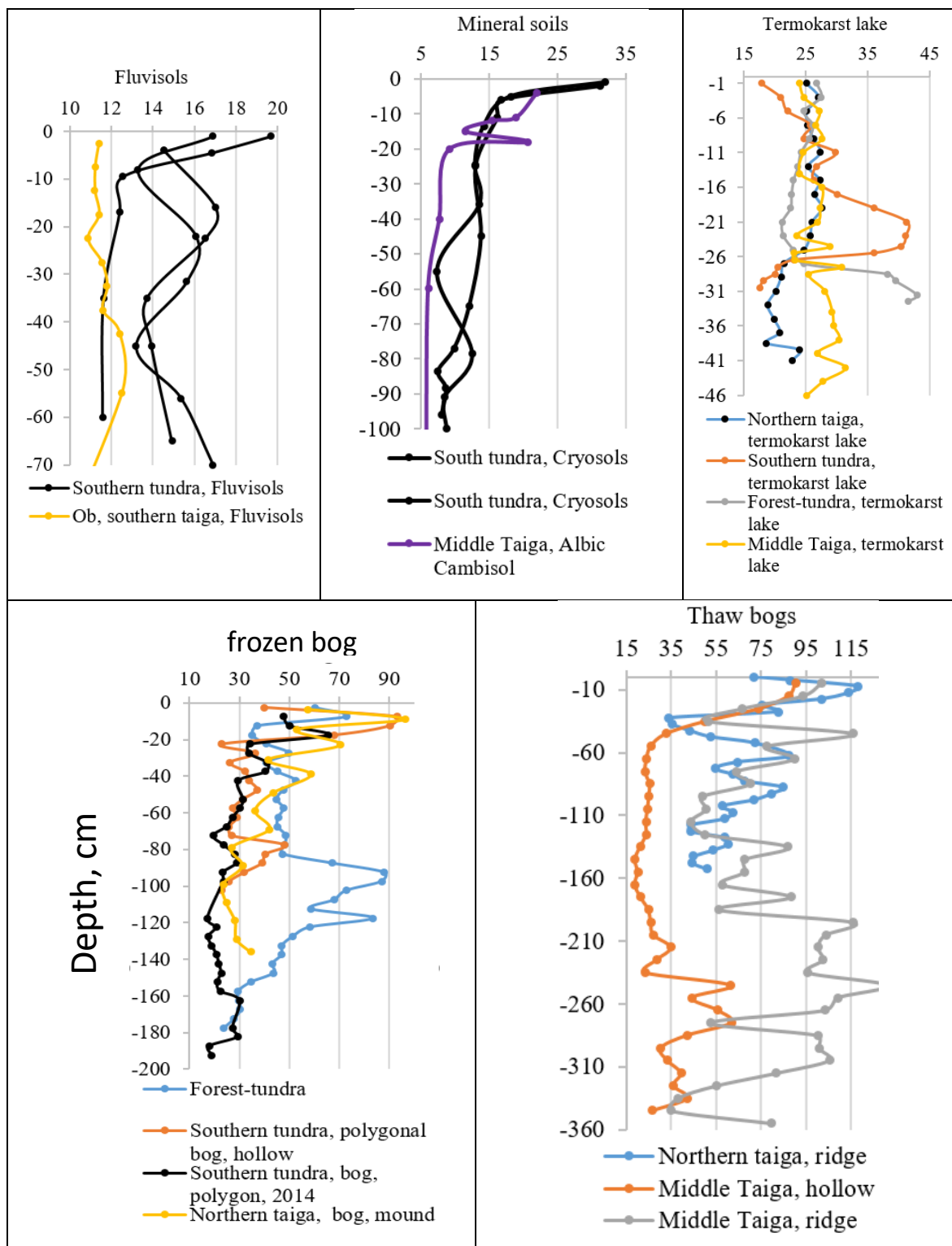


999

1000 **Fig. S4.** Seasonally-resolved export fluxes of particulate C, N, P and RSM from WSL rivers
1001 during spring (May and June), summer (July and August) and autumn (September and
1002 October) for permafrost-free region and 4 distinct permafrost zones.

1003

1004



1005

1006

1007 **Fig. S5.** C:N in peat profile across the latitudinal transect of WSL, corresponding to four main
 1008 regions (permafrost-free region of Ob, southern taiga; isolated/sporadic permafrost at Kogalym;
 1009 discontinuous permafrost at Khanymey and continuous permafros at Tazovsky). Authors'
 1010 unpublished data.